The Plant Cell, Vol. 16, 2984–3001, November 2004, www.plantcell.org

The Arabidopsis CSN5A and CSN5B Subunits Are Present in Distinct COP9 Signalosome Complexes, and Mutations in Their JAMM Domains Exhibit Differential Dominant Negative Effects on Development

Giuliana Gusmaroli, Suhua Feng, and Xing Wang Deng[1]

Department of Molecular, Cellular, and Developmental Biology, Yale University, New Haven, Connecticut 06520-8104

The COP9 signalosome (CSN) is an evolutionarily conserved multisubunit protein complex involved in a variety of signaling and developmental processes through the regulation of protein ubiquitination and degradation. A known biochemical role attributed to CSN is a metalloprotease activity responsible for the derubylation of cullins, core components for several types of ubiquitin E3 ligases. The CSN's derubylation catalytic center resides in its subunit 5, which in *Arabidopsis thaliana* is encoded by two homologous genes, *CSN5A* and *CSN5B*. Here, we show that CSN5A and CSN5B subunits are assembled into distinct CSN complexes in vivo, which are present in drastically different abundances, with CSN^{CSN5A} appearing to be the dominant one. Transgenic CSN5A and CSN5B proteins carrying a collection of single mutations in or surrounding the metalloprotease catalytic center are properly assembled into CSN complexes, but only mutations in CSN5A result in a pleiotropic dominant negative phenotype. The extent of phenotypic effects caused by mutations in CSN5A is reflected at the molecular level by impairment in Cullin1 derubylation. These results reveal that three key metal binding residues as well as two other amino acids outside the catalytic center play important roles in CSN derubylation activity. Taken together, our data provide physiological evidence on a positive role of CSN in the regulation of Arabidopsis SCF (for Skp1-Cullin-F-box) E3 ligases through RUB (for Related to Ubiquitin) deconjugation and highlight the unequal role that CSN^{CSN5A} and CSN^{CSN5B} play in controlling the cellular derubylation of cullins. The initial characterization of *CSN5A* and *CSN5B* insertion mutants further supports these findings and provides genetic evidence on their unequal role in plant development.

INTRODUCTION

The COP9 signalosome (CSN) is a highly conserved multiprotein complex that was originally identified as a negative regulator of plant photomorphogenesis (Wei et al., 1994a). In response to a changing light environment, a complex network of signaling pathways integrate light, nutritional, and hormonal signals to coordinate the expression of an array of genes involved in the regulation of growth and development. In the absence of light, photomorphogenic development is repressed and *Arabidopsis thaliana* seedlings undergo an alternative developmental program (skotomorphogenesis or etiolation) characterized by elongated hypocotyls and closed and unexpanded cotyledons. By virtue of their inability to undergo etiolation (constitutively photomorphogenic) and their dark purple seed coat color (fusca), a group of *constitutively photomorphogenic/de-etiolated/fusca* (*cop/det/fus*) mutants was isolated (Castle and Meinke, 1994; Miséra at al., 1994; Wei et al., 1994b; Wei and Deng, 1996). Besides the constitutive photomorphogenic phenotype, null *cop/det/fus* mutants also display severe abnormalities in overall development that lead to lethality after the seedling stage.

Six of the nine molecularly characterized *COP/DET/FUS* loci encode six of the eight subunits of CSN (Wei et al., 1994b; Staub et al., 1996; Karniol et al., 1999; Serino et al., 1999; Peng et al., 2001a). The remaining two CSN subunits, CSN5 and CSN6, are not represented by any of the *COP/DET/FUS* loci because they are encoded by two small gene families, each composed of two genes (Kwok et al., 1998; Peng et al., 2001b). The subsequent identification of the CSN in many other eukaryotic organisms revealed the conservation of this complex throughout evolution (Chamovitz et al., 1996; Seeger et al., 1998; Freilich et al., 1999; Karniol et al., 1999; Mundt et al., 1999; Busch et al., 2003). Interestingly, six of the eight subunits of the CSN contain a PCI (for Proteasome, COP9, Initiation factor 3) domain, whereas the other two (CSN5 and CSN6) contain a MPN/MOV34 (for Mpr1p and Pad1p N-terminal) domain (Aravind and Ponting, 1998; Hofmann and Bucher, 1998; Ponting et al., 1999). PCI and MPN domains are also found in two other large protein complexes: the eukaryotic translation Initiation factor 3 (eIf3) and the lid subcomplex of the 26S proteasome (Glickman et al., 1998; Hofmann and Bucher, 1998; Wei et al., 1998; Wei and Deng, 1999; Fu et al., 2001). Whereas eIf3 is involved in protein translation, the 26S proteasome is a protein degradation machinery highly conserved in eukaryotes.

[1] To whom correspondence should be addressed. E-mail xingwang.deng@yale.edu; fax 203-432-5726.

The author responsible for distribution of materials integral to the findings presented in this article in accordance with the policy described in the Instruction for Authors (www.plantcell.org) is: Xing Wang Deng (xingwang.deng@yale.edu).

Article, publication date, and citation information can be found at www.plantcell.org/cgi/doi/10.1105/tpc.104.025999.

The major known biochemical role assigned to CSN is the removal of the ubiquitin-like protein RUB (for Related to Ubiquitin; also called NEDD8) from the cullin subunit of the cullin-containing E3 ligases (Lyapina et al., 2001; Zhou et al., 2001). It also deubiquitinates cullins, possibly through association with Ubp12 (Groisman et al., 2003; Zhou et al., 2003). Among E3 ligases, the SCF (for Skp1-Cullin-F-box) group represents a major subclass of the multisubunit RING containing E3 ubiquitin ligase superfamily (Deshaies, 1999; Vierstra, 2003; Smalle and Vierstra, 2004). A typical SCF complex consists of a cullin family member, Cullin1 (CUL1), a small ring finger protein (RBX1/ROC1/HRT1), a SKP1-like adaptor, and an F-box protein that confers the specificity for the recruitment of the substrate. Cullins can be covalently modified by RUB, but usually only a small fraction of CUL1 is found in the rubylated form. However, *csn* mutants from yeast, *Drosophila melanogaster*, and Arabidopsis accumulate exclusively rubylated CUL1 (Lyapina et al., 2001; Schwechheimer et al., 2001; Doronkin et al., 2002). Besides CUL1, CSN also deconjugates RUB from other cullins, including CUL2 and CUL3 (Zhou et al., 2001; Yang et al., 2002; Pintard et al., 2003), and regulates the activity of the recently identified CUL4-containing E3 ligase complexes (Groisman et al., 2003). Like the ubiquitin pathway, the RUB conjugation pathway is catalyzed by enzymatic cascade and is essential in *Schizosaccharomyces pombe*, *Caenorhabditis elegans*, Drosophila, and mouse (Jones and Candido, 2000; Osaka et al., 2000; Tateishi et al., 2001; Ou et al., 2002; Lykke-Andersen et al., 2003). Rubylation also plays an important role in many plant processes including embryo development and auxin and ethylene responses (del Pozo et al., 2002; Dharmasiri et al., 2003; Larsen and Cancel, 2004).

The RUB modification of the cullin subunit is highly dynamic and thought to regulate the E3 ligase activity. In fact, rubylation is an important positive regulator of cullin ubiquitin ligases by facilitating substrate polyubiquitination and E2 recruitment to the SCF (Wu et al., 2000; Kawakami et al., 2001). As RUB modification stimulates cullin-containing E3 ligase activity in vitro, derubylation by CSN should in theory inhibit SCF function. Despite biochemical data demonstrating that CSN negatively regulates cullin activity in vitro (Yang et al., 2002; Groisman et al., 2003; Zhou et al., 2003), genetic evidence suggests that CSN promotes cullin-dependent substrate degradation in vivo. Arabidopsis transgenic lines with reduced CSN function show an impaired degradation of IAA6 protein, a likely substrate of SCF^{TIR1} (Schwechheimer et al., 2001). Likewise, in *S. cerevisiae*, deletion of *CSN5* exacerbates the growth defect of a temperature-sensitive allele of *SCF* mutants, delaying the degradation of SIC1 (Cope et al., 2002), whereas in *S. pombe*, CSN1 and CSN2 are required for the CUL4-dependent ubiquitination and degradation of SPD1 (Liu et al., 2003). This apparent paradox suggests that active cycles of rubylation and derubylation are required to properly sustain the activity of the SCF complexes (Schwechheimer and Deng, 2001; Cope and Deshaies, 2003; Wei and Deng, 2003; Wolf et al., 2003). Thus, CSN potentially influences a tremendous number of cellular pathways that together contribute to the pleiotropic phenotype of CSN mutants and their lethality in Drosophila (Freilich et al., 1999; Doronkin et al., 2002; Oron et al., 2002; Suh et al., 2002) or Arabidopsis (Wei and Deng, 1992; Wei and Deng, 1996).

The biochemical basis of the CSN-associated derubylation activity has been recently linked to the metalloprotease motif ($EX_nHXHX_{10}D$) of CSN5, which is embedded within the larger MPN domain known as the JAMM (JAB1/MPN/Mov34) or MPN+ motif (Cope et al., 2002; Maytal-Kivity et al., 2002). Similarly, the same motif in RPN11 has been implicated in the deubiquitination activity of the proteasome lid (Verma et al., 2002; Yao and Cohen, 2002). In addition, a ubiquitin isopeptidase activity requiring an intact CSN5 JAMM domain also has been described in mammalian cells (Groisman et al., 2003). Nevertheless, CSN5 or RPN11 protein alone are inactive in the absence of association with CSN or the proteasome, respectively. Recently, the crystal structure of an *Archaeoglobus fulgidus* JAMM domain–containing protein (AF2198) has been determined, which confirmed that a zinc ion was present in the catalytic center (Tran et al., 2003; Ambroggio et al., 2004). However, the CSN5-dependent metalloprotease activity is not essential in fission yeast, where no obvious phenotype has been detected in the *csn5* mutant (Zhou et al., 2001; Mundt et al., 2002).

To date, the physiological importance of the CSN5-JAMM motif has been established only in Drosophila, where point mutations in the JAMM metal binding site arrest development at the larvae stage, with abnormalities in photoreceptor neuron differentiation (Cope et al., 2002). In this study, we demonstrate that CSN5A and CSN5B are incorporated into distinct CSN complexes, with only one copy of subunit 5 present in each complex. Moreover, we show that identical point mutations in several conserved residues within CSN5A and CSN5B JAMM/MPN domains differentially affect CUL1 derubylation in vivo and correlate with the severity of the associated phenotype. The initial characterization of *CSN5A* and *CSN5B* insertion mutants provides genetic evidence in support of these findings. Taken together, these data indicate that CSN^{CSN5A} and CSN^{CSN5B} complexes play unequal roles in plant development, with CSN^{CSN5A} as the major player in the regulation of CUL1-based SCF E3 ligases, and highlight the physiological relevance of an intact JAMM domain and its associated derubylation activity in Arabidopsis.

RESULTS

Identification of *csn5b* T-DNA Insertion Mutant

In Arabidopsis, two conserved genes, named *CSN5A* and *CSN5B*, encode two isoforms of the subunit 5 of CSN (Kwok et al., 1998). The two genes (At1g22920 and At1g71230) are located on the opposite arms of chromosome one. Sequence analyses indicated that CSN5A and CSN5B share 86 and 88% identity at the nucleotide (cDNA) and protein levels, respectively. To assess the physiological function of the two distinct CSN5 isoforms, we screened the available T-DNA and transposon collection databases for insertional mutations in the *CSN5* loci. A T-DNA insertion within the *CSN5B* locus was identified from the SALK collection (Figure 1A). Heterozygous T1 plants carrying the T-DNA insertion allele show a 3:1 segregation ratio of kanamycin resistant:kanamycin sensitive in T2 progeny, indicating that one single T-DNA insertion locus is present in this mutant line. PCR-based genotype analyses revealed that the T-DNA is inserted

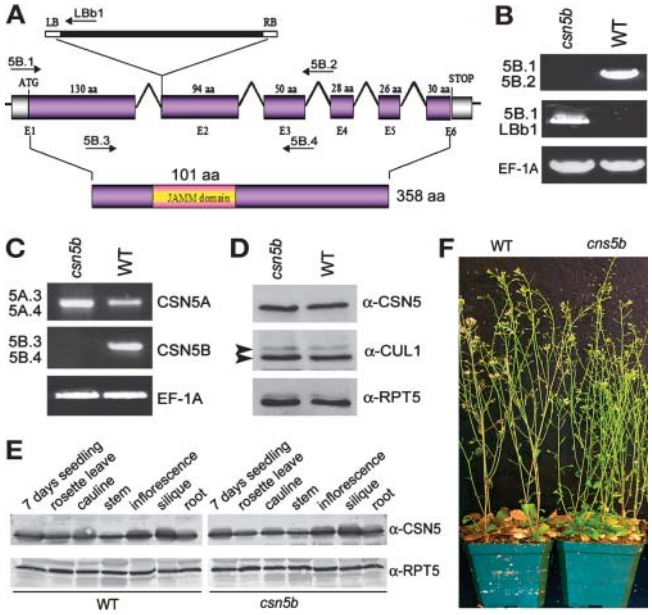

Figure 1. Identification and Characterization of the Arabidopsis *csn5b* T-DNA Insertion Mutant.

(A) Structure of the Arabidopsis *CSN5B* locus (At1g71230) and graphic representation of the T-DNA insertion. Exons are represented by violet and gray (untranslated regions) boxes, and introns are represented by lines. Arrows schematically represent the position and orientation of the gene-specific primers (5B.1, 5B.2, 5B.3, and 5B.4) and the left border T-DNA specific primer (LBb1) used for the molecular analyses. aa, amino acids.

(B) PCR-based genotype analyses of Arabidopsis *csn5b* homozygous mutant and wild-type plants. Primers 5B.1 and 5B.2 were used to specifically amplify the *CSN5B* wild-type allele; primers 5B.1 and LBb1 were used to specifically amplify the *csn5b*::*T-DNA* insertion allele. The genomic sequence of the *EF-1A* locus was used as positive control for the PCR reactions.

(C) Detection of *CSN5A* and *CSN5B* specific transcripts in 2-week-old *csn5b* homozygous mutant and wild-type seedlings by RT-PCR. Primers 5B.3 and 5B.4 were used to specifically amplify the *CSN5B* cDNA, and primers 5A.3 and 5A.4 (see Figure 9) were used to specifically amplify the *CSN5A* cDNA. As positive control for the RT-PCR reactions, gene-specific primers were used to amplify the *EF-1A* cDNA.

(D) Detection of CSN5 proteins in 2-week-old *csn5b* homozygous mutant and wild-type Arabidopsis seedlings. Total proteins were subjected to SDS-PAGE and immunoblot analyses with α-CSN5 and α-CUL1 polyclonal antibodies. Equal protein loads were confirmed by immunoblot analyses with α-RPT5 (a proteasome ATPase subunit) polyclonal antibody. The α-CSN5 antibody recognizes both CSN5A/CSN5B isoforms. Arrowheads indicate rubylated and unrubylated CUL1, respectively.

(E) Detection of CSN5 protein in wild-type and *csn5b* homozygous plants. Total proteins extracts were prepared from the indicated tissues, subjected to SDS-PAGE, and immunoblotted with α-CSN5 antibody. Equal protein loads were confirmed with α-RPT5 antibody.

(F) Arabidopsis wild type and *csn5b* mutant show similar phenotype when grown under identical conditions.

within the first intron of the *CSN5B* gene and identified homozygous mutant plants in the T2 progeny (Figure 1B). RT-PCR analyses of the homozygous T-DNA insertion *csn5b* mutants show the complete lack of the *CSN5B* transcript (Figure 1C). This result suggests that the homozygous T-DNA insertion in the *CSN5B* locus results in a null mutant.

Null *csn5b* Mutants Do Not Display Observable Phenotype and Alteration in the Ratio of Rubylated/Unrubylated CUL1

As shown in Figure 1D, α-CSN5 polyclonal antibody detects a single band migrating around 42 kD both in wild-type and *csn5b* null mutant extracts. Because the α-CSN5 antibody recognizes both CSN5A and CSN5B isoforms (Kwok et al., 1998), it is evident that the band detected in null *csn5b* extract corresponds to CSN5A. Because a major biochemical activity of CSN is the removal of RUB from the cullins, we examined whether the lack of the CSN5B subunit could influence the rubylation status of CUL1. As shown in Figure 1D, no difference has been observed in the ratio of rubylated/unrubylated CUL1 in wild-type and *csn5b* seedling protein extracts. To test if CSN5A and CSN5B might play differential roles in a tissue-specific manner, wild-type and *csn5b* protein extracts obtained from different organs at various developmental stages were blotted against α-CSN5 and α-CUL1 antibodies, respectively. As shown in Figure 1E, CSN5A was detected at high levels in all the organs analyzed, with no apparent difference being observed between wild-type and *csn5b* homozygous plants. Similarly, no significant differences were observed in the rubylated/unrubylated ratio of CUL1 in these samples (data not shown). The absence of a biochemical effect on CUL1 rubylation correlates with the observation that *csn5b* null mutants display a wild-type phenotype. In fact, when grown in the dark, *cns5b* homozygous seedlings undergo normal skotomorphogenesis. In normal light growth conditions, *csn5b* mutants are fertile and do not exhibit any detectable abnormality throughout the whole life span (Figure 1F).

CSN5A Is Present in Both CSN and Subcomplex Forms

In gel filtration analyses of Arabidopsis wild-type seedlings, the CSN5 subunits elute in high molecular mass fractions and cofractionate with the other CSN subunits. The elution peak is roughly centered between 450 and 550 kD and corresponds to the CSN complex (Kwok et al., 1998). Besides the CSN peak, a portion of CSN5 can be found in a lower molecular mass form of ~100 to 150 kD and cofractionates with a subset of other CSN subunits, which includes CSN3 (data not shown). The existence of two discrete CSN5 forms has been shown in mammalian cells, Drosophila (Oron et al., 2002; Yang et al., 2002), and in fission yeast (Zhou et al., 2001; Mundt et al., 2002). Whereas the CSN holocomplex is predominantly nuclear localized, the smaller CSN5 forms are cytoplasmic in both mammals (Tomoda et al., 2002) and Arabidopsis (Kwok et al., 1998). However, the precise physiological role of CSN5 free-form and its link to CSN biochemical functions are still unclear.

To investigate if the lack of CSN5B could influence the chromatographic elution properties of the CSN5 complex forms in vivo, we compared the gel fractionation profiles of wild-type

(data not shown) and *csn5b* seedlings (Figure 2A). The CSN5A elution profile of *csn5b* mutant extracts is identical to that of the wild type. These data indicate that CSN5B is not required for the assembly and stability of the CSN5A-containing CSN holocomplex and that CSN5A participates in the CSN holocomplex as well as in the lower molecular mass form.

CSN5A-myc and CSN5B-myc Fusion Proteins Incorporate Properly into CSN in Vivo

To further define the qualitative and quantitative contributions of the two CSN5 subunits in the formation of CSN, we expressed epitope-tagged CSN5A or CSN5B in the *csn5b* null mutant background. Both CSN5A and CSN5B were fused in frame to nine copies of the myc epitope-tag (myc_9) at their C termini. The chimeric *CSN5A-myc* and *CSN5B-myc* transgenes, driven by the 35S promoter of *Cauliflower mosaic virus*, were transformed into the homozygous *csn5b* mutants, and T2 transgenic lines expressing recombinant CSN5A-myc and CSN5B-myc at comparable levels were chosen for further investigation (see Methods for details; Figures 4C, lane 3, CSN5A-myc, and 4D, lane 2, CSN5B-myc). Protein blot analyses of gel filtration fractions using α-myc antibody indicate that both CSN5A-myc and CSN5B-myc fusion proteins elute in high molecular mass fractions (elution peak from fractions 12 to 15; Figures 2B and 2C) and overlap with other CSN subunits. These results suggest that the presence of the myc_9-tag at the C termini of CSN5A and CSN5B does not interfere with their ability to efficiently incorporate into the CSN complex. Moreover, when ectopically expressed in transgenic seedlings, both CSN5A-myc and CSN5B-myc participate in the formation of CSN and the lower molecular mass form (Figures 2B and 2C). The elution peaks of the CSN complex and the lower molecular mass form containing CSN5A-myc (Figure 2B) and CSN5B-myc (Figure 2C) are slightly shifted toward larger molecular mass fractions compared with those containing endogenous CSN5A. This shift is likely attributable to the presence of the myc_9-epitope that increases the masses of those CSN5-containing complexes.

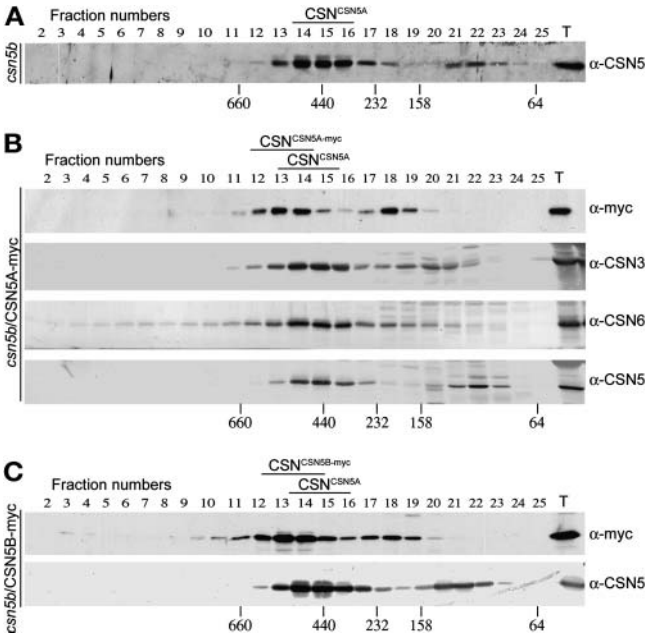

Figure 2. The CSN5A-myc and CSN5B-myc Fusion Proteins Properly Incorporate into CSN in Transgenic Plants.

Immunoblot analyses of Superose 6 gel filtration fractions obtained from 2-week-old light-grown *csn5b* **(A)**, *csn5b*/35S:CSN5A-myc **(B)**, and *csn5b*/35S:CSN5B-myc **(C)** transgenic Arabidopsis seedlings. Column fractions were subjected to SDS-PAGE and probed with α-myc 9E10, α-CSN5, α-CSN3, and α-CSN6 antibodies. Fraction numbers are indicated. Lane T contains the total unfractionated extracts. Recombinant CSN5A-myc and CSN5B-myc cofractionate with other CSN subunits as $CSN^{CSN5A\text{-}myc}$ and $CSN^{CSN5B\text{-}myc}$ complexes (elution pick from fractions 12 to 15) that are slightly bigger then the CSN complex containing untagged CSN5A (CSN^{CSN5A}) (elution pick from fractions 13 to 16). The shift is attributable to the presence of the myc_9 epitope tag in CSN5A-myc and CSN5B-myc, respectively.

CSN5A and CSN5B Are Present within Distinct CSN Complexes Each Containing Only One Copy of CSN5

We further tested whether both CSN5A and CSN5B can integrate into the same CSN, or if they participate in the formation of distinct populations of CSN complexes. In either case, we were also interested in defining the copy number of the CSN5 subunit within each CSN complex. To address these questions, we took advantage of Arabidopsis *csn5b* plants expressing CSN5A-myc and CSN5B-myc. First, immunoprecipitation of the CSN complex was performed on protein extracts obtained from *csn5b*/35S:CSN5B-myc transgenic seedlings using an α-myc affinity matrix (Figure 3A). In this line, endogenous CSN5A and recombinant CSN5B-myc proteins are both expressed, as shown in Figure 4D (lane 2). The stringency of the immunoprecipitation was optimized to purify only the core CSN complex and avoid the coimmunoprecipitation of secondary interacting proteins as a result of complex–complex interactions (e.g., CSN-CSN, CSN-SCFs, or CSN-proteasome; Peng et al., 2003). Under this stringent immunoprecipitation of CSN, the α-myc matrix could efficiently pull down the CSN5B-myc fusion protein and copurify all the other components of the $CSN^{CSN5B\text{-}myc}$, but not the endogenous CSN5A or other interacting proteins, such as CUL1 (Figure 3A). In control immunoprecipitation experiments, we did not observe any nonspecific precipitation of the CSN subunits from wild-type (Figure 3A) or *csn5b* (data not shown) extracts by the α-myc matrix. This result indicates that CSN5B-myc and endogenous CSN5A are present in distinct CSN complexes, even though they presumably coexist in the same tissue.

We further performed immunoprecipitation of CSN from protein extracts of *csn5b*/35S:CSN5A-myc transgenic seedlings. Again, endogenous CSN5A and recombinant CSN5A-myc proteins in this line are both expressed, as shown in Figure 4C (lane 3). If two or multiple copies of CSN5A were present in the same CSN complex, we would expect to obtain the copresence of CSN5A-myc and CSN5A in the same immunoprecipitation. As shown in Figure 3B, the α-myc beads could pull down the CSN5A-myc fusion protein and copurify the other subunits of CSN but not the endogenous CSN5A or the CUL1 subunit of the SCF complex (Figure 3B). Again, we did not detect any

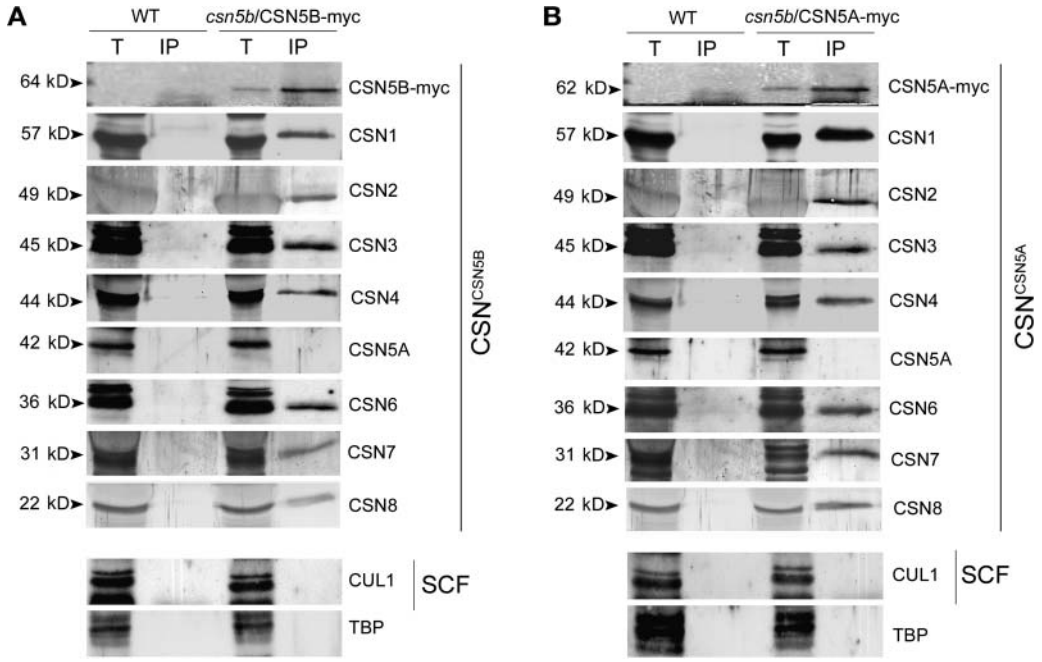

Figure 3. The Arabidopsis CSN5A and CSN5B Are Incorporated into Distinct CSN Complexes in Vivo.

(A) Immunoprecipitation of the CSN^{CSN5B} complex from transgenic Arabidopsis *csn5b* seedlings stably expressing CSN5B-myc. Seedling protein extracts prepared from 2-week-old wild-type and *csn5b*/35S:CSN5B-myc transgenic lines were used.

(B) Immunoprecipitation of the CSN^{CSN5A} complex from transgenic Arabidopsis *csn5b* seedlings stably expressing CSN5A-myc. Seedling protein extracts prepared from 2-week-old wild-type and *csn5b*/35S:CSN5A-myc transgenic lines were used.

The immunoprecipitates and the total extracts were subjected to SDS-PAGE and immunoblotted with antibodies against myc, CSN1, CSN2, CSN3, CSN4, CSN5, CSN6, CSN7, CSN8, and CUL1. Lane T indicates the total protein extracts. Lane IP indicates the immunoprecipitates with α-myc 9E10 antibody immobilized onto Sepharose fast flow beads matrix (9E10 affinity matrix). α-TBP (TATA binding protein) antibody is used as a pull-down negative control. Data are representative of three independent experiments.

nonspecific precipitation of the CSN subunits from wild-type (Figure 3B) or *csn5b* (data not shown) proteins extracts. This result indicates that CSN5A and CSN5A-myc do not coexist in the same CSN complex.

Taken together, these data suggest that CSN5A and CSN5B are present in distinct complexes. In the case of CSN5A, only one CSN5 subunit seems to be present within each CSN complex. Thus, at least two forms of CSN exist in Arabidopsis, one containing CSN5A, and the other one CSN5B. We designate these complexes as CSN^{CSN5A} and CSN^{CSN5B}.

Stable Expression of a Series of Point Mutations within or Around the Metal Binding Motif of CSN5A and CSN5B in Arabidopsis

The presence of two distinct CSN complexes (CSN^{CSN5A} and CSN^{CSN5B}) raises a question about their relative contribution toward the overall CSN function in the regulation of protein degradation. As a way to define their biological function in vivo, we created a series of identical point mutations in or surrounding the JAMM metal binding motif and expressed these mutated versions as myc-tagged fusion proteins in the *csn5b* mutant background. It has been previously shown that point mutations of either two conserved His residues or an Asp residue within the putative metal binding motif ($EX_nHXHX_{10}D$) of the CSN5-JAMM domain disrupt CSN derubylation activity in yeast without interfering with the assembly of the complex (Cope et al., 2002). In Arabidopsis, these residues correspond to H142, H144, and D155 and are conserved in both CSN5A and CSN5B proteins (Figures 4A and 4B). Site-specific mutagenesis was used to convert H142 and H144 into Ala (H142A and H144A) and D155 into Asn (D155N) in both Arabidopsis CSN5A and CSN5B subunits. Interestingly, a Cys residue (C149) is present within a conserved stretch of amino acids that exhibit a striking similarity with the consensus of the Cys box, the catalytic site of the Cys-based proteases (Hochstrasser, 1996). However, point mutation of this corresponding Cys residue into Ala in CSN5 failed to eliminate the derubylation in yeast (Zhou et al., 2001). To test its importance in Arabidopsis, we mutated the conserved Cys into Ala (C149A) in both CSN5A and CSN5B subunits. An additional C149S substitution was introduced into CSN5A. In addition, the sequence alignment of MPN-containing proteins highlights the presence of an Asp residue (D175 in Arabidopsis) that is conserved in CSN5/RPN11 orthologs (Figure 4B). Thus, we also introduced two different point mutations, converting D175 into Glu (D175E) and Asn (D175N), respectively, in both CSN5A and CSN5B proteins. All the single CSN5A and CSN5B amino acid substitutions are summarized in Tables 1 and 2, respectively.

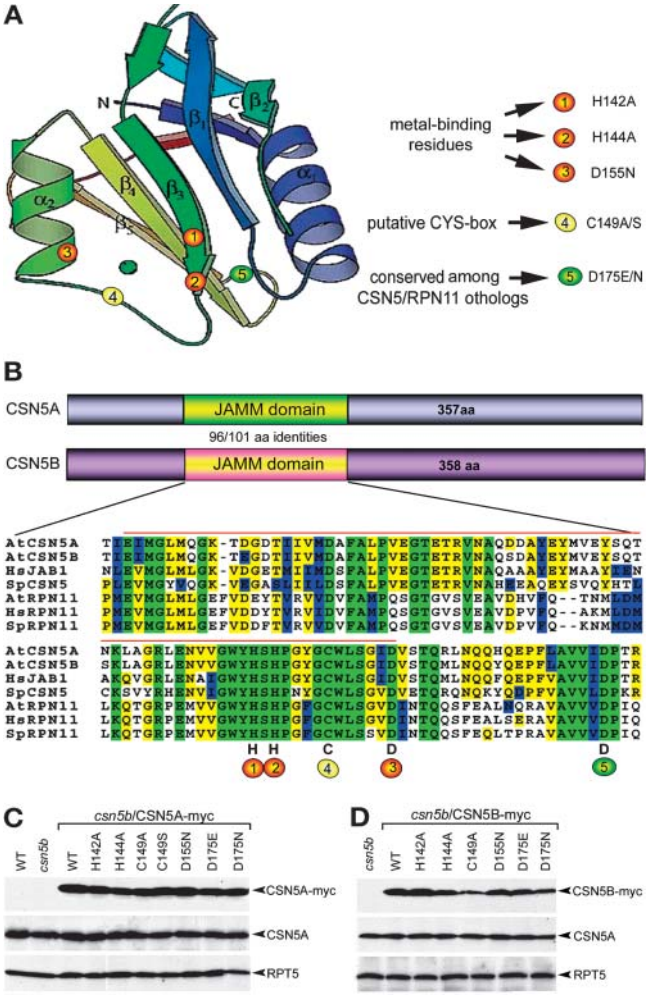

Figure 4. Ectopic Expression of the JAMM Point-Mutated CSN5A/CSN5B Variants in Transgenic Arabidopsis Seedlings.

(A) Graphic representation of the tertiary structure of the JAMM domain protein AF2198 obtained from Tran et al. (2003). The illustration has been slightly modified from its original version to point out the positions of the single CSN5A/CSN5B amino acid substitutions in the context of the putative tertiary structure of the CSN5 JAMM domain.

(B) Schematic representation of Arabidopsis CSN5A and CSN5B subunits and alignment of the JAMM domains of yeast, human, and Arabidopsis CSN5/RPN11 orthologs. Selected sequences were aligned using ClustalW and modified manually to ensure correct superposition of the conserved motif. The metal binding motif within the JAMM domain is marked by an orange line on top. aa, amino acids.

(C) and **(D)** Immunoblot analyses of protein extracts obtained from 10-d-old *csn5b* transgenic seedlings expressing the complete series of wild-type and mutated CSN5A-myc transgenes **(C)** or the complete series of wild-type and mutated CSN5B-myc transgenes **(D)**. Protein extracts from 10-d-old wild-type and *csn5b* seedlings were used as controls. The protein blots were probed with α-myc and α-CSN5 antibodies. α-RPT5 antibody is used as a loading control.

As shown in Figure 4, the α-myc antibody detects a single band of the expected size for the fusion proteins in total extracts of *csn5b* null mutant transformed with the complete series of wild-type and mutated CSN5A-myc (Figure 4C) and CSN5B-myc (Figure 4D) transgenes (see Methods for details). In addition to the expression of the CSN5A-myc and CSN5B-myc transgenes, all the transgenic lines used in this study express endogenous CSN5A at a level comparable to that of wild-type plants (Figures 4C and 4D). Transgenic *csn5b* plants expressing the wild-type CSN5A-myc and CSN5B-myc transgenes described above were used as control in all subsequent analyses.

Point Mutations in CSN5A and CSN5B Do Not Interfere with the Integrity and Stability of CSN^{CSN5A} and CSN^{CSN5B} in Vivo

To ascertain whether the point mutations in the CSN5A and CSN5B subunits interfere with their ability to assemble into the CSN^{CSN5A} and CSN^{CSN5B} complexes, respectively, we performed cofractionation analyses of the complete series of mutated CSN5A-myc and CSN5B-myc transgenes. As shown in Figure 5A, protein blot analyses using α-myc antibody indicate that all the mutated CSN5A-myc (Figure 5A) and CSN5B-myc (Figure 5B) fusion proteins elute in high molecular mass fractions (elution peak from fractions 12 to 15; Figure 5) and cofractionate with the other CSN subunits (data not shown). This observation is consistent with previous studies in *S. pombe*, in which single point mutations in the conserved His and Asp (Arabidopsis H142, H144, and D155) do not interfere with the assembly of the yeast CSN complex (Cope et al., 2002). The results shown in Figure 5 also point out that other single amino acid substitutions in key residues located inside (C149A and C149S for CSN5A and C149A for CSN5B) or outside (D175E and D175N for both CSN5A and CSN5B) the zinc binding motif of the JAMM/MPN domain do not appear to alter the ability of the mutated proteins to assemble into stable CSN complexes. In all cases, protein blot analyses using the α-CSN5 antibody indicate that endogenous CSN5A does not cofractionate with the CSN5A-myc and CSN5B-myc containing CSN complexes (data not shown), in agreement with the finding that only one subunit 5 is present within each CSN complex (Figure 3).

Several CSN5A Point Mutations Confer a Partial Photomorphogenic Phenotype in the Dark

Because all the *COP/DET/FUS* loci have been originally identified by virtue of their inability to undergo etiolation in darkness, we first examined the transgenic lines expressing wild-type and mutated CSN5A-myc and CSN5B-myc fusion proteins for possible photomorphogenic phenotypes. Remarkably, four distinct point mutations of CSN5A (H142A, H144A, C149S, and D175N) confer a dominant and partial photomorphogenic phenotype to 4-d-old dark-grown *csn5b* null mutant seedlings (Figure 6A). However, this phenotype is not present at 100% among the homozygous progenies, likely because of a different degree of penetrance of the dominant CSN5A mutations. To test whether the observed traits correlated with the derubylation activity of CSN, protein extracts from those 4-d-old dark-grown seedlings were subjected to immunoblot analysis using α-CUL1 antibody.

Table 1. Summary of CSN5A Wild-Type and Mutant Proteins Expressed in Arabidopsis *csn5b* Plants

Transgene	Original Amino Acid	Position	Converted into	Myc Fusion in CSN Complex[a]	Impaired CUL1 Derubylation[b]	Phenotype at Late Flowering Stage	Penetrance Rate
CSN5A	Wild type	–[c]	–	Yes	No	Wild type	–
CSN5A-H142A	His	142	Ala	Yes	Yes	Very severe	80–100%
CSN5A-H144A	His	144	Ala	Yes	Yes	Severe	60–70%
CSN5A-C149A	Cys	149	Ala	Yes	No	Slightly reduced height	10%
CSN5A-C149S	Cys	149	Ser	Yes	Yes	Severe	50–60%
CSN5A-D155N	Asp	155	Asn	Yes	Yes	Severe	70–90%
CSN5A-D175E	Asp	175	Asn	Yes	Yes	Severe	60%
CSN5A-D175N	Asp	175	Glu	Yes	Yes	Very severe	80–100%

[a] The proper assembly of the CSN5A-myc fusion proteins into CSN complex in vivo was evaluated by gel filtration and protein blot analyses.
[b] The impaired derubylation activity of CSN was determined by monitoring the in vivo rubylation level of Arabidopsis CUL1.
[c] Wild-type amino acids at each given position.

As shown in Figures 6A and 6B, a striking correlation exists between the accumulation of rubylated CUL1 (RUB-CUL1) and the appearance of the photomorphogenic phenotype (e.g., line *csn5b*/35S:CSN5A-H144A-myc). Interestingly, when grown in the light, H142A and D175N T2 lines segregate a variable number of hyperphotomorphogenic seedlings characterized by the accumulation of a higher level of anthocyanin in the cotyledons and petiole, compared with wild-type seedlings grown under the same conditions (Figure 6C). All the purple seedlings produce green true leaves after seedling stage. It is important to note that neither the mutant nor the wild-type CSN5B transgenes caused any detectable photomorphogenic phenotype.

Most Point Mutations in CSN5A but Not CSN5B Differentially Affect Growth and Development at the Vegetative Phase

To further dissect the specific role of each point mutation in both CSN5A and CSN5B subunits, we analyzed the effect of the dominant negative mutant transgenes at different stages of Arabidopsis growth and development. At vegetative phase, after seedling stage but before bolting, all the CSN5A-myc mutant transgenic lines (with the exception of C149A) have rosettes smaller than the wild type, with shorter petioles and curled leaves, as shown in Figures 6D (right) and 6F. Notably, this phenotype is not present in transgenic plants expressing the wild-type CSN5A-myc or CSN5B-myc subunits, or any CSN5B-myc mutants. The curled leaves and short petiole phenotypes exhibit a different degree of severity, depending on each given transgene. At this phase, mutation of Cys 149 causes the weakest effects. In fact, although the CSN5A-C149A mutant plants do not display any observable phenotype, plants expressing CSN5A-C149S exhibit a smaller rosette and shorter petioles compared with wild-type and *csn5b*/35S:CSN5A-myc plants (Figure 7C). The CSN5A-C149S mutation displays a penetrance of ~60% (e.g., only 60% of the progeny with the transgene exhibits the phenotype). On the other hand, expression of CSN5A-H142A-myc and CSN5A-D175N-myc proteins cause an extremely severe phenotype in essentially 100% of progeny. Transgenic plants carrying either one of those mutant CSN5A subunits developed into very small rosettes with extremely short petioles and unusually curled leaves (Figure 7C). The D155N, H144A, and D175E mutations in CSN5A exhibit an intermediate degree of severity (Figure 7C; data not shown) and a phenotypic penetrance between 60 and 90%.

Table 2. Summary of CSN5B Wild-Type and Mutant Proteins Expressed in Arabidopsis *csn5b* Plants

Transgene	Original Amino Acid	Position	Converted into	Myc Fusion in CSN Complex[a]	Impaired CUL1 Derubylation[b]	Phenotype at Late Flowering Stage
CSN5B	Wild type	–[c]	–	Yes	No	Wild type
CSN5B-H142A	His	142	Ala	Yes	No	Wild type
CSN5B-H144A	His	144	Ala	Yes	No	Wild type
CSN5B-C149A	Cys	149	Ala	Yes	No	Wild type
CSN5B-D155N	Asp	155	Asn	Yes	No	Wild type
CSN5B-D175E	Asp	175	Asn	Yes	No	Wild type
CSN5B-D175N	Asp	175	Glu	Yes	No	Wild type

[a] The proper assembly of the CSN5B-myc fusion proteins into CSN complex in vivo was evaluated by gel filtration and protein blot analyses.
[b] The impaired derubylation activity of CSN was determined by monitoring the in vivo rubbylation level of Arabidopsis CUL1.
[c] Wild-type amino acids at each given position.

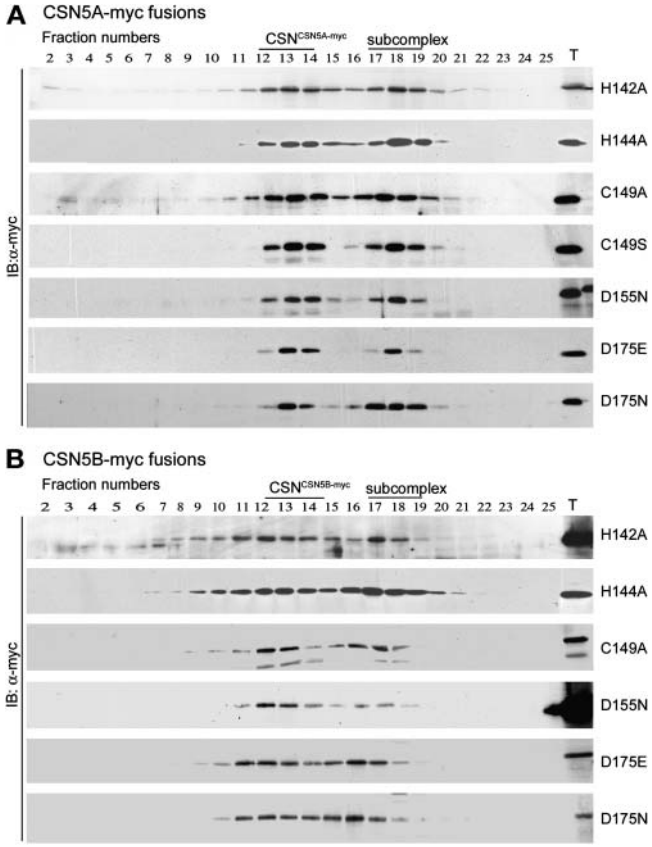

Figure 5. Different Point mutations of Arabidopsis CSN5A and CSN5B Do Not Interfere with CSN^{CSN5A} and CSN^{CSN5B} Complex Formation in Vivo.

(A) Protein blot analyses of Superose 6 gel filtration fractions obtained from 2-week-old light-grown *csn5b* Arabidopsis seedlings expressing the complete series of CSN5A point-mutated transgenes. Column fractions were subjected to SDS-PAGE and probed with α-myc antibody. All of the mutated CSN5A-myc variants eluted as $CSN^{CSN5A\text{-}myc}$ complex (elution peak in fractions 12 to 15) as well as in lower molecular mass forms (fractions 17 to 19).

(B) Protein blot analyses of Superose 6 gel filtration fractions obtained from 2-week-old light-grown *csn5b* Arabidopsis seedlings expressing the complete series of CSN5B point-mutated transgenes. Column fractions were subjected to SDS-PAGE and probed with α-myc antibody. All of the point-mutated CSN5B-myc variants eluted as $CSN^{CSN5B\text{-}myc}$ complex (elution peak in fractions 12 to 15) as well as in lower molecular mass forms (fractions 17 to 18).

The Severity of the Phenotype Caused by Point-Mutated CSN5A Proteins Correlates with the Level of in Planta CUL1 Rubylation

To test whether the dominant phenotype of the transgenic CSN5A mutant plants could be attributed to the impaired derubylation activity of the endogenous $COP9^{CSN5A}$ signalosome, we examined the AtCUL1 modification pattern of each transgenic line by protein blot analysis of total protein extracts (Figures 6G and 6H). To further ascertain whether RUB-CUL1 accumulates as monomer or in the context of SCF complexes, the same protein extracts shown in Figures 6G and 6H were subjected to gel filtration analyses (Figures 6I to 6L). With the only exception of CSN5A-C149A that does not display any phenotype at the vegetative stage, all the other CSN5A mutant proteins interfered to various degrees with the derubylation activity of endogenous CSN^{CSN5A}, as evidenced by the higher level of accumulation of RUB-modified CUL1 in the SCF complex fractions (Figures 6G and 6L). This correlation appears to be quantitative, in the sense that a higher RUB-CUL1 level corresponds with a more severe phenotype. Remarkably, the corresponding mutations in CSN5B (Figures 6H and 6K) or overexpression of wild-type CSN5A-myc and CSN5B-myc proteins (Figure 6J) did not affect the derubylation activity of endogenous $COP9^{CSN5A}$, which is consistent with the absence of phenotype in those transgenic plants. This is despite the fact that all those fusion proteins were efficiently incorporated into CSN complexes in vivo (Figures 2C, 2D, and 5B). In all cases, the gel filtration profiles indicate that elevated RUB-CUL1 accumulates in the context of SCF complexes but not in the monomeric form (Figures 6I to 6L).

All Point-Mutated *CSN5A-myc* (but Not *CSN5B-myc*) Transgenes Result in Developmental Defects at the Reproductive Phase

At the reproductive phase, the phenotype of the transgenic CSN5A-myc mutant plants becomes even more drastic (Figure 7D), as summarized in Table 1. However, none of the transgenic lines expressing the corresponding mutations in the CSN5B or control proteins (wild-type CSN5B-myc in Figure 7A or CSN5A-myc in Figure 7B, left) displayed any notable phenotype and are virtually indistinguishable from wild-type plants. At this phase, all of the *CSN5A-myc* mutant transgenes result in an evident reduction in the overall plant size (Figure 7). Although the CSN5A-C149A mutation did not cause any detectable phenotype at vegetative phase, it also resulted in mild dwarfism at this late stage (Figure 7B). All the other CSN5A mutations (including C149S) exhibit a severe dwarfism (Figure 7D), accompanied by an increase in the number of secondary inflorescences (Figure 8A) and leaves (Figure 8B). The outgrowth of the secondary inflorescences in wild-type plants is inhibited by the apical dominance of the primary shoot apex through the production of the plant hormone auxin. It has already been shown that plants with reduced CSN levels have decreased auxin response (Schwechheimer et al., 2001). Therefore, the phenotypic traits of the transgenic CSN5A mutant plants likely result from a reduction of the overall CSN activity at this development stage.

Another striking aspect of the phenotype is a dramatic reduction in the internode length and in the size and architectures of the primary and secondary inflorescences (Figures 8C to 8H). In fact, whereas in wild-type plants, the secondary branches emerge at regular intervals from the primary shoot (Figure 8E, left), transgenic CSN5A mutant plants display a severe disorganization in the whole aerial architecture because of a defect in the timing of organ initiation and in organ size control (Figure 8E, right). Moreover, cauline leaves, flower buds (Figure 8G), as well

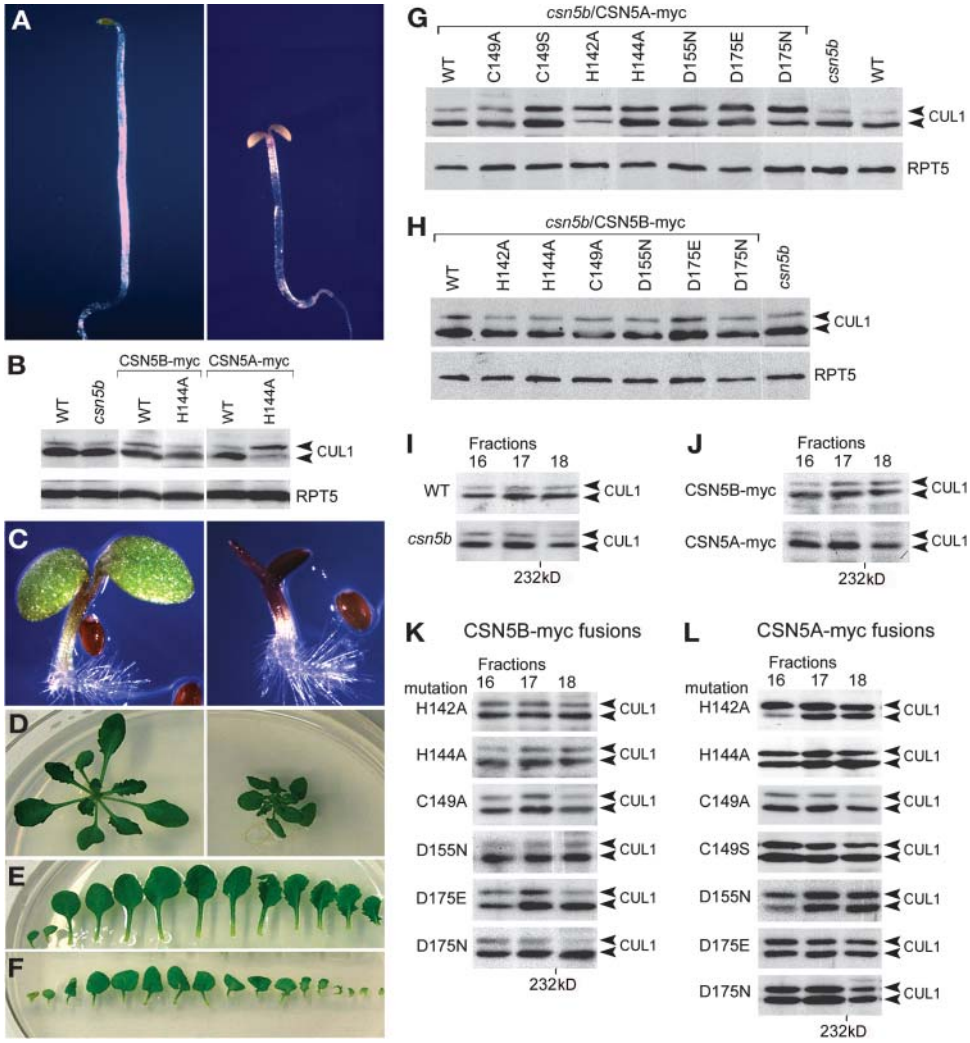

Figure 6. Dominant Negative Point Mutations in the Arabidopsis CSN5A (but Not CSN5B) Subunit Differentially Affect Photomorphogenesis and Early Development in a Manner Correlating with Impaired CUL1 Derubylation in Vivo.

(A) Partial photomorphogenic phenotype of 4-d-old dark-grown Arabidopsis *csn5b* seedlings expressing CSN5A-H144A-myc (right) with the control 4-d-old, dark-grown *csn5b* seedling expressing CSN5B-H144A-myc (left). The seedling in the left panel displays the same phenotype of 4-d-old, dark-grown, wild-type seedlings.

(B) Protein blot analyses of protein extracts obtained from 4-d-old *csn5b* transgenic seedlings expressing the wild-type CSN5A-myc, wild-type CSN5B-myc, CSN5A-H144A-myc, and CSN5B-H144A-myc. Protein extracts from 4-d-old, dark-grown wild-type and *csn5b* seedlings were used as controls. The blots were probed with α-CUL1 antibody. α-RPT5 antibody was used as loading control. The arrowheads indicate the position of rubylated and unrubylated CUL1, respectively.

(C) Light-grown 6-d-old Arabidopsis *csn5b* seedlings expressing either CSN5B-H142A-myc (left) or CSN5A-H142A-myc (right). The seedling on the left, expressing the CSN5B-H142A-myc transgene, displays a phenotype identical to that of the wild type.

(D) Morphology of 3-week-old light-grown *csn5b* plants expressing either CSN5B-H142A-myc (left) or CSN5A-H142A-myc (right). The plant on the left, expressing the CSN5B-H142A-myc transgene, displays a phenotype identical to that of the wild type.

(E) and **(F)** Leaf and petiole phenotypes of *csn5b* plants expressing either CSN5B-H142A-myc **(E)** or CSN5A-H142A-myc **(F)**.

(G) and **(H)** Protein blot analyses of total protein extracts from 3-week-old *csn5b* plants expressing the wild-type and mutated CSN5A-myc transgenes **(G)** or the wild-type and mutated CSN5B-myc transgenes **(H)**. Protein extracts from 3-week-old wild-type and *csn5b* plants, grown in the same conditions, were used as controls. The protein blots were probed with α-CUL1 antibody. The α-RPT5 antibody was used as a loading control. The arrowheads indicate the position of rubylated and unrubylated CUL1, respectively.

(I) to **(L)** Protein blot analyses of Superose 6 gel filtration fractions from plants described in **(G)** and **(H)**. Column fractions were subjected to SDS-PAGE and probed with α-CUL1 antibody. The CUL1 subunit elutes as high molecular mass form corresponding to the SCF (fractions 16 to 18) according to a molecular weight roughly centered around 300 kD. The arrowheads indicate the position of rubylated and unrubylated CUL1, respectively.

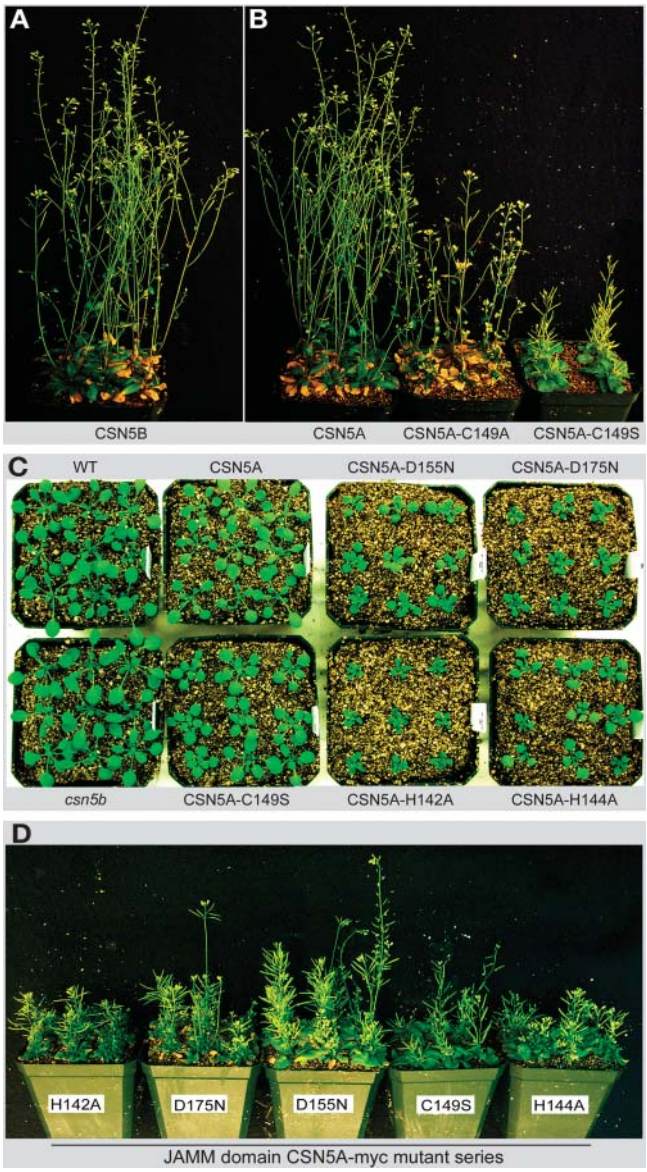

Figure 7. Distinct Point Mutations in the Arabidopsis CSN5A Catalytic Domain Differentially Affect Vegetative and Reproductive Development.

(A) Seven-week-old *csn5b* Arabidopsis plants carrying *35S:CSN5B-myc* display the wild-type phenotype.

(B) Effect of two different amino acid substitutions on C149 during reproductive development. Seven-week-old Arabidopsis *csn5b* plants overexpressing wild type CSN5A-myc (left), CSN5A-C149A-myc (middle), and CSN5A-C149S-myc (right).

(C) Comparison of morphological defects of 3-week-old light-grown plants.

(D) Comparison of the pleiotropic phenotypes of five point mutations in the CSN5A JAMM domain at reproductive phase (7 weeks old).

as mature flowers (Figure 8I) are smaller in the dominant CSN5A mutant lines than in wild-type plants, whereas the secondary inflorescences are drastically altered in their overall size and structure because of the complete failure of internodes to elongate (Figures 8D, 8F, and 8H).

Finally, whereas in wild-type plants, the siliques are spaced at regular intervals around the inflorescence stem, in CSN5A-myc mutated lines, the position, orientation, size, and morphology of the siliques are drastically altered (Figure 8C). In general, all the lines expressing mutant CSN5A proteins display distinctive curled leaves (Figures 8J to 8L) and wavy siliques (Figures 8N to 8P), characterized by the presence of irregular bump and roughness on their surfaces. These morphological abnormalities are reflected at the cellular level by a dramatic change in leave and silique cell shape and length, as shown by scanning electron microscopy (Figures 8M and 8Q).

Once again, protein blot analyses of transgenic protein extracts at this developmental stage confirmed the expression of both the recombinant (CSN5A-myc or CSN5B-myc) and endogenous CSN5A subunits in all wild-type and mutated CSN5A/CSN5B-myc transgenic lines (data not shown). This result indicates that the phenotype of the transgenic plants described above results from a dominant negative action of point-mutated CSN5A proteins and not from a general cosuppression mechanism.

The Initial Characterization of a Recessive *csn5a* Mutation Supports an Unequal Role Played by CSN5A and CSN5B on Plant Development

In our continued effort of screening the available Arabidopsis insertional mutant collections, a T-DNA insertion line for the *CSN5A* locus was identified from a newly released SALK collection. PCR-based genotyping analyses revealed that the T-DNA is inserted within the last intron (Figure 9A). Protein blot analysis of the homozygous mutant plants (Figure 9B) shows that unlike the wild type, where a single band is present, two bands are detected in *csn5a* homozygous mutants (Figure 9C). In *csn5a* mutants, the larger band is the same size as in wild type (42 kD), but much less abundant, and should correspond to the CSN5B subunit. The fast migrating band (~36 kD) observed only in the *csn5a* mutants most likely corresponds to the truncated CSN5A protein (Figures 9A and 9C). Gel filtration analyses revealed that the wild-type CSN5B protein is assembled into the CSN^{CSN5B} complex in vivo, whereas the truncated CSN5A protein does not cofractionate with the CSN holocomplex (data not shown).

The segregation analysis indicates that this T-DNA insertion resulted in a recessive *csn5a* mutation. Only the homozygous *csn5a* mutants exhibit a pleiotropic phenotype, which is strikingly reminiscent of many aspects of the phenotypes caused by expression of the dominant CSN5A JAMM point mutations. Those phenotypes include partial photomorphogenic development of dark-grown seedlings (Figure 9E), hyperphotomorphogenic development of light-grown seedlings (Figure 9F), curled and small rosette leaves, dwarfed stature, and the loss of apical dominance (Figure 9G). The *csn5a* homozygous mutant plants also accumulate a higher ratio of rubylated CUL1 compared with the wild type (Figure 9D). The fact that the *csn5b* mutant does not exhibit any observable phenotype, whereas the *csn5a* mutant does, once again indicates that CSN5A plays a more prominent role in plant development.

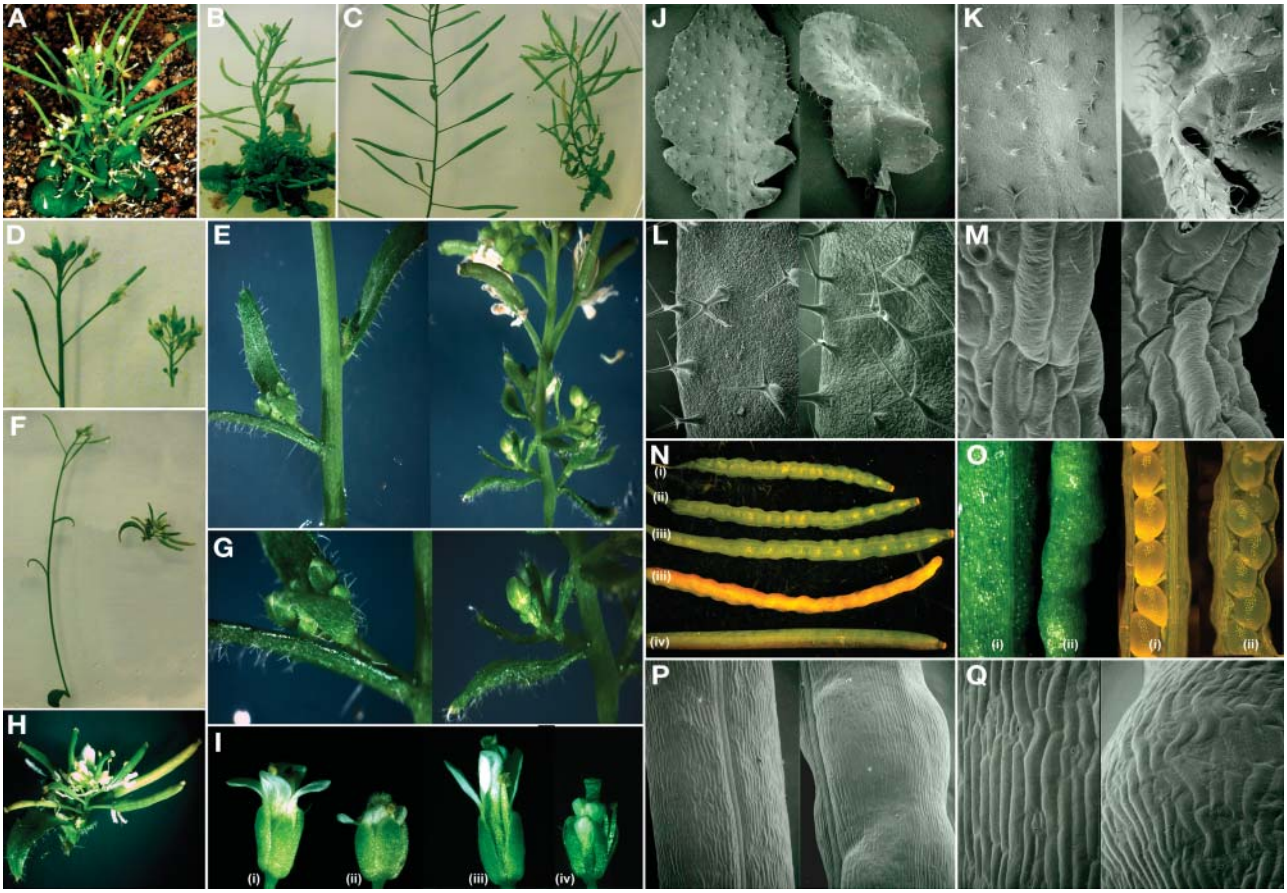

Figure 8. Multifaceted Developmental Defects of *csn5b* Plants Expressing Point-Mutated CSN5A Proteins.

(A) Phenotype induced by the dominant mutation CSN5A-D175N in 6-week-old *csn5b* transgenic plants.
(B) Phenotype induced by the dominant mutation CSN5A-H142A in 6-week-old *csn5b* transgenic plants.
(C) Primary inflorescences of 6-week-old wild-type (left) and *csn5b*/CSN5A-D155N-myc (right) plants.
(D), **(F)**, and **(H)** Secondary inflorescences of 6-week-old wild-type (**[D]** and **[F]**, left) and *csn5b*/CSN5A-H144A (**[D]**, **[F]**, right, and **[H]**) plants.
(E) and **(G)** Close-up images of primary inflorescences from 5-week-old wild-type (left) and *csn5b*/CSN5A-C149S-myc (right) plants. Pictures in the same panel were taken with the same magnification.
(I) Stereomicroscopic images of wild-type (i and iii) and *csn5b*/CSN5A-D175N-myc (ii and iv) flowers at 1 (i and ii) and 3 (iii and iv) d after pollination.
(J) to **(M)** Scanning electron microscopy images of rosette leaves from wild-type (left) and *csn5b*/CSN5A-D175N-myc transgenic (right) plants. Pictures in the same panel were taken with the same magnification.
(N) Stereomicroscopic images of siliques from *csn5b*/CSN5A-H142A-myc (i), *csn5b*/CSN5A-D175N-myc (ii), *csn5b*/CSN5A-C149S-myc (iii), and wild-type (iv) plants.
(O) Stereomicroscopic images of siliques from wild-type (i) and *csn5b*/CSN5A-D175N-myc (ii) plants.
(P) and **(Q)** Scanning electron microscopy images of siliques from wild-type (left) and *csn5b*/CSN5A-D175N-myc (right) plants. Pictures in the same panel were taken with the same magnification.

DISCUSSION

Arabidopsis Has Distinct CSN Complexes Containing Either CSN5A or CSN5B as Subunit 5

Arabidopsis is the only species known to have two genes encoding the subunit 5 of the CSN (Kwok et al., 1998). The presence of two CSN5 isoforms raises an evident question concerning their structural and functional distinction and similarity. By the stable expression of CSN5A-myc and CSN5B-myc fusion proteins in a *csn5b* null mutant background, we were able to definitively show that CSN5A and CSN5B are present within distinct CSN complexes in vivo, which we designated CSN^{CSN5A} and CSN^{CSN5B}, respectively.

In the case of CSN5B-myc transgenic plants, the coexistence of the endogenous CSN5A and the CSN5B-myc in the cell does not lead to the incorporation of the two proteins into the same CSN complex, as shown in Figures 2C and 3A. Instead, two different complexes, CSN^{CSN5A} and $CSN^{CSN5B\text{-}myc}$, are evidently formed. This result indicates that CSN5A and CSN5B do not

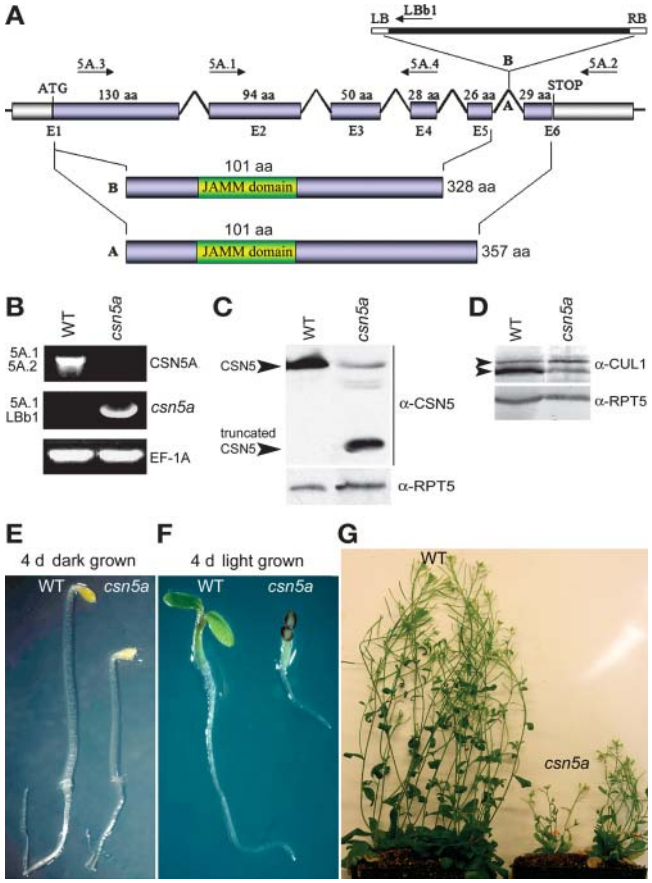

Figure 9. Initial Characterization of a Recessive *csn5a* Insertion Mutant.

(A) Structure of the Arabidopsis *CSN5A* locus (At1g22920) and graphic representation of the T-DNA insertion. Exons are represented by blue (coding region) and gray (untranslated regions) boxes, and introns are represented by single lines. Arrows schematically represent the location of the gene-specific primers (5A.1, 5A.2, 5A.3, and 5A.4) and the left border T-DNA specific primer (LBb1) used for the molecular analyses. The wild-type and presumed truncated CSN5A proteins are illustrated.

(B) PCR-based genomic analyses of Arabidopsis *csn5a* homozygous mutant and wild-type plants. Primers 5A.1 and 5A.2 have been used to specifically amplify the *CSN5A* wild-type allele; primers 5A.1 and LBb1 were used to specifically amplify the *csn5a*::*T-DNA* insertion allele. The genomic sequence of the *EF-1A* locus was used as positive control for the PCR reactions.

(C) and **(D)** Detection of CSN5 **(C)** and CUL1 **(D)** proteins in 2-week-old *csn5a* homozygous mutant and wild-type Arabidopsis seedlings. Total proteins were subjected to SDS-PAGE and immunoblot analyses with α-CSN5 **(C)** and α-CUL1 **(D)** polyclonal antibodies. Arrowheads indicate rubylated and unrubylated CUL1, respectively. Equal protein loads were confirmed using α-RPT5 antibody.

(E) Phenotype of 4-d-old, dark-grown, wild-type and *csn5a* seedlings.

(F) Phenotype of 4-d-old, light-grown, wild-type and *csn5a* seedlings.

(G) Pleiotropic phenotype of 6-week-old *csn5a* mutant plant. Six-week-old wild-type plant is shown as control.

participate in the formation of the same CSN complex. In the same way, in the case of CSN5A-myc transgenic lines, the coexistence of the endogenous CSN5A subunit and the recombinant CSN5A-myc in the cell does not lead to the copresence of those two proteins within the same CSN complex, as shown in Figures 2B and 3B. Indeed, once again, two distinct complexes, CSN^{CSN5A} and $CSN^{CSN5A\text{-}myc}$, are formed. This last finding indicates that the CSN complex does not contain two or more copies of the same CSN5A subunit. This conclusion might have general implications for the structural relationship between multiple CSN isoforms in other organisms.

Arabidopsis CSN^{CSN5A} and CSN^{CSN5B} Play Unequal Roles in Development

The fact that *CSN5A* and *CSN5B* have so far escaped the saturation screens aimed to identify CSN loss-of-function mutants led to the assumption of a functional redundancy of those two CSN5 isoforms (Serino and Deng, 2003). However, two *CSN5* genes have been reported only in Arabidopsis and in other members of the plant kingdom, but not in fission yeast, Drosophila, and in all the vertebrates so far analyzed. This raises the question of why plants would need two CSN5 subunits. Besides showing their participation in distinct CSN complexes, in this study, we presented genetic and biochemical evidences of the unequal roles played by those two subunits in the overall CSN functions.

An evaluation of CSN5A protein levels in different organs at selected developmental stages (Figure 1E) reveals that CSN5A is by far the predominantly expressed subunit in all organs analyzed. This observation is consistent with the microarray analyses of the expression level of those two *CSN5* genes in more than 17 organ types. In all cases, *CSN5A* is expressed at a significant higher level in all the tissues and cell types examined (our unpublished data). The same conclusion can also be reached by examining the expression profiles of *CSN5A* and *CSN5B* obtained from Geneinvestigator (http://www.genevestigator.ethz.ch), which collected hundreds of microarray expression data sets. In all the organs and conditions so far reported, *CSN5A* is consistently expressed at a much higher level than *CSN5B*. On this basis, it is reasonable to assume that between the two Arabidopsis CSN5 subunits, CSN5A plays the major role. This assumption is clearly supported by the fact that the complete loss of the entire CSN5B subunit (homozygous *csn5b* insertion line) does not result in any obvious morphologic and biochemical defect (Figure 1), whereas, on the contrary, the deletion of 29 amino acids at the C-terminal of CSN5A results in a severe pleiotropic phenotype (Figures 9E to 9G), similar to those of the CSN5A mutant transgenic plants, even in the presence of wild-type CSN5B protein (Figure 9C). The latest observation implies that CSN5A and CSN5B are not functionally equal.

This notion is also consistent with the fact that all the point mutations in key residues within or around the CSN5A metal binding motif exert a dominant negative effect on plant development, whereas the corresponding point mutations in CSN5B do not, as summarized in Figure 10. The fact that all the mutated CSN5A-myc and CSN5B-myc forms are properly integrated into full-size CSN as well as in smaller subcomplexes in vivo (Figure 5) suggests that either the mutated $CSN^{CSN5A\text{-}myc}$

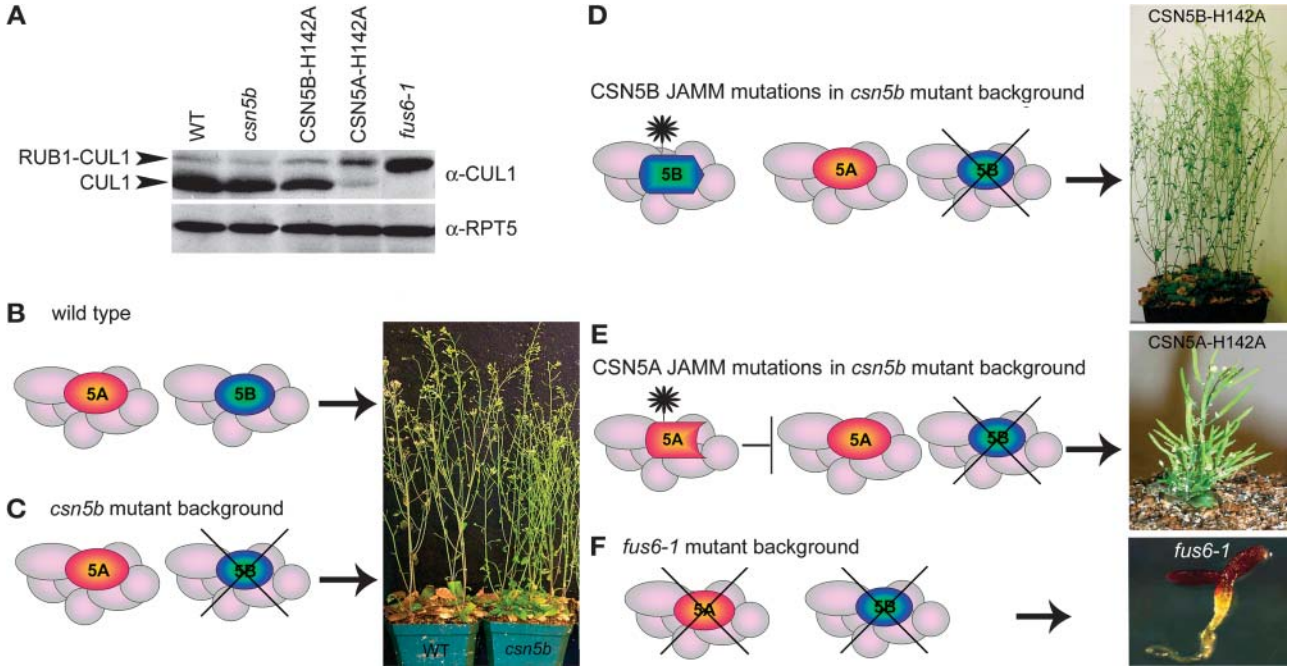

Figure 10. Schematic Summary of the Effects of Different CSN-Related Arabidopsis Lines on CUL1 Rubylation Level and Growth Phenotype.

(A) Protein blot analyses of protein extracts from 10-d-old Arabidopsis seedlings. The blots were probed with α-CUL1 antibody. The α-RPT5 antibody was used as a loading control. The arrowheads indicate the positions of rubylated and unrubylated CUL1, respectively. A null *csn* mutant (*fus6-1*) accumulates only rubylated CUL1. CSN5A transgenic plants expressing point mutations in the CSN5A JAMM domain accumulate mainly rubylated CUL1 (e.g., *csn5b*/CSN5A-H142A), whereas the corresponding point mutations of CSN5B protein (e.g., *csn5b*/CSN5B-H142A) or the *csn5b* null mutation do not affect CUL1 rubylation level.

(B) to **(F)** Diagrams illustrate the activity of the CSN complexes and the phenotypic effects of their mutations on plant development. The point mutations in the JAMM domains of CSN5A or CSN5B were labeled with a starlet. Although the complete loss of the entire CSN5B subunit does not cause any obvious morphological defect under normal growth conditions (cf. **[B]** and **[C]**), single point mutations in CSN5A are sufficient to induce severe developmental defects **(E)**. The pleiotropic phenotype of the dominant CSN5A mutations correlates with the accumulation of mainly rubylated CUL1, as shown in **(A)**. The corresponding point mutations in CSN5B do not negatively affect growth and development **(D)** or the rubylation status of CUL1 **(A)**. The complete loss of function of CSN in a null *csn* mutant **(F)** causes lethality after seedling stage and accumulation of CUL1 exclusively in the rubylated form **(A)**.

complexes or the subcomplexes containing mutated CSN5A-myc can interfere with the function of the endogenous CSN^{CSN5A}. Conversely, the mutated $CSN^{CSN5B\text{-}myc}$ complexes, or the subcomplexes containing mutated CSN5B-myc, are not capable of interfering with the activity of the endogenous CSN^{CSN5A}. These observations once again imply unequal roles for CSN5A and CSN5B in the regulation of Arabidopsis development. The detailed characterization of our recently identified *csn5a* homozygous mutant, as well as the double *csn5a csn5b* mutant, will provide useful information about the precise role of the CSN5A and CSN5B subunits in specific cell types or regulatory pathways. However the observations that *csn5b* null mutants are perfectly viable, fertile, and do not display any obvious abnormalities indicate that the CSN^{CSN5A} per se is sufficient to sustain all the functions attributed to the CSN. On the other hand, the formation of a truncated CSN5A protein results in a pleiotropic phenotype that is less severe than the phenotype reported for the null *csn* mutants (Wei et al., 1994a; Serino and Deng, 2003). This suggests that even if CSN^{CSN5B} alone is not able to sustain the normal plant development, its activity might be responsible for the lack of a lethal *fusca* phenotype in the *csn5a* mutants.

Both the Residues within and around the Metal Binding Motif of CSN5A Play Critical Roles in CSN's Derubylation Activity

On the bases of their diverse degree of penetrance and severity, we could infer a different level of strength to each CSN5A amino acid substitution. We noted that C149A has a relatively minor effect on the overall plant size and does not interfere significantly with CUL1 derubylation at vegetative phase, which is in agreement with previous findings in yeast, where C149A did not eliminate the deneddylation activity of CSN5 (Zhou et al., 2001). However, we show that mutation of this Cys into Ser (C149S) causes a small rosette/short petiole phenotype at vegetative phase (Figure 7C) and leads to a higher level of accumulation of rubylated CUL1. Both mutations result in an observable phenotype at the later reproductive phase, even though the conversion of Cys into Ser has a more severe effect, as shown in Figure 7B. On the bases of the JAMM crystal structure (Figure 4A, modified from Tran et al. (2003), the conserved Cys lays on a hydrophobic groove on the protein's surface close to the catalytic zinc ion and could potentially be involved in substrate binding. Similarly, point mutations of D175 into Asn (D175N) and H142 into Ala (H142A)

trigger a severe phenotype (Figure 7C), defining these two amino acid substitutions with the best penetrance. Whereas H142 is one of the three residues involved in the coordination of the catalytic zinc ion (H142, H144, and D155), D175 lays at the 3′ edge of the JAMM domain, within a loop located on the opposite site of the tertiary structure of the active metalloprotease center (Figure 4A). The observation that mutations in the other two residues involved in the coordination of the zinc ion (H144A and D155N) have less penetrance than D175N clearly indicates the very critical role played by this aspartic residue in the regulation of the proteolytic activity of CSN^{CSN5A}. Taken together, our data point at the existence of a specific mechanism by which only point mutations in CSN5A can interfere with the derubylation activity of endogenous CSN^{CSN5A} complex.

A Tight Correlation between CSN's Derubylation Activity and Its Ability to Modulate Arabidopsis Development

By monitoring the rubylation status of CUL1, we could establish a strong correlation between the increased levels of rubylated cullin and the appearance of the pleiotropic phenotype in all transgenic plants examined (Figure 10). It is important to note how all the major aspects of the pleiotropic phenotype of the point-mutated CSN5A lines described in this study are strikingly similar to those exhibited by CSN5 cosuppression lines (Schwechheimer et al., 2001), which was caused by a drastic decrease in the cellular CSN level. In fact, all the salient features of the CSN5A mutated plants are remarkably similar to the crucial aspects of the CSN5 cosuppression lines, including a partial dark-grown photomorphogenic phenotype, curled small rosette, and a notable increase in the number of secondary inflorescences accompanied by a general reduction in plant size and internode length. The CSN5 cosuppression plants preferentially accumulate rubylated CUL1 and have been shown to be impaired in the degradation of PSIAA6, a candidate substrate of the SCF^{TIR1} E3 ligases (Schwechheimer et al., 2001). Thus, the reduction of the cellular CSN5 levels in those transgenic lines leads to a decreased auxin response, similar to loss-of-function mutants of the E3 ubiquitin ligase SCF^{TIR1}. The observation that the phenotype of the transgenic CSN5A mutant lines is also remarkably similar to that of the *csn5a* C-terminal deletion mutant (Figure 9) further supports the notion that CSN^{CSN5A} plays the major role in the regulation of SCF^{TIR1} and that the expression of point-mutated CSN5A subunits causes a dominant negative effect on the activity of the endogenous CSN^{CSN5A}. Finally, the fact that the severity of the phenotype of those transgenic plants correlates with the extent of accumulation of rubylated CUL1 reveals a clear link between the derubylation activity of CSN and its ability to modulate plant development. However, it is important to point out that the CUL1 derubylation defects do not always correlate with the severity of the *csn* mutant phenotype. Arabidopsis plants containing a mutant CSN complex with N-terminal deletion in CSN1 ($CSN^{CSN1\text{-}C231}$) displayed a wild-type pattern of CUL1 rubylation. Nevertheless, the CSN1-C321 mutation was lethal and exhibited severe gene expression defects (Wang et al., 2002). On the other hand, in *S. pombe*, although deletion of all of the CSN subunits resulted in hyperrubylation of Pcu1, only *Δcsn1* and *Δcsn2* display growth defects (Zhou et al., 2001; Mundt et al., 2002). Those observations would imply that there are other essential activities of CSN independent from the derubylation of cullins.

Although CSN^{CSN5A} plays a major role in the auxin-mediated response possibly through the regulation of SCF^{TIR1}, many aspects of the pleiotropic phenotype described in Figure 8 (including a reduction in the flower size and changes in leaf and silique morphologies) cannot be solely explained by impaired SCF^{TIR1} functions. Because the Arabidopsis genome encodes ~700 F-box containing proteins (Serino and Deng, 2003), an impressive number of combinatorial possibilities could account for the formation of hundreds of alternative CUL1-based SCF E3 ligase complexes. Thus, a combination of defects in multiple SCF ligases could potentially influence a tremendous amount of cellular pathways and eventually lead to the pleiotropic phenotype observed in the transgenic lines. This notion is supported by the fact that several E3 ligases, including SCF^{TIR1} (Gray et al., 1999), SCF^{COI1} (jasmonic acid response; Xu et al., 2002), and SCF^{UFO} (flower development; Samach et al., 1999; Zhao et al., 2001) are known to interact with CSN in vivo (Schwechheimer et al., 2001; Feng et al., 2003; Wang et al., 2003). This is also consistent with the observation that transgenic plants with reduced RBX1 levels (Gray et al., 2002; Schwechheimer et al., 2002) share a remarkable number of morphological defects with the CSN5A mutated plants described in this study, suggesting that the CSN^{CSN5A} might be involved in the regulation of several types of RBX1-based E3 ligases.

Many aspects, if not all, of the developmental defects observed in transgenic plant carrying point mutations in the JAMM domain of CSN5A are strikingly similar to that observed in transgenic plants overexpressing a dominant negative version of ECR1 (del Pozo et al., 2002). Because ECR1 encodes a subunit of the heterodimeric RUB-activating enzyme (E1), the dominant version of ECR1 negatively affects the rubylation pathway, resulting in a reduction of the RUB conjugation to CUL1. The astonishing similarity between ECR1 and CSN5A dominant negative lines points out that cycles of rubylation/derubylation are required for the proper functions of the SCF ubiquitin ligases in vivo and once again indicates that CSN^{CSN5A} is the major player in the derubylation of Arabidopsis CUL1.

METHODS

Plant Materials and Growth Conditions

The wild-type *Arabidopsis thaliana* plants used in this study are the Columbia-0 ecotype. The T-DNA Insertion lines in *CSN5A* and *CSN5B* were identified in the Salk collection (lines Salk_027705 for CSN5A and Salk_007134 for CSN5B, mistakenly reported as insertion in *CSN5B* and *CSN5A*, respectively). The homozygous insertion lines were isolated through PCR-based genotyping and named *csn5a* and *csn5b*. All the transgenic lines used in this study were obtained by direct transformation of the wild type and mutated recombinant CSN5A and CSN5B proteins into the *csn5b* homozygous background. The *fus6-1* mutant has been described previously (Castle and Meinke, 1994; Miséra et al., 1994; Pepper et al., 1994; Wei et al., 1994b). The Arabidopsis seeds were surface sterilized and the plants grown on solid 1× MS medium supplemented with 1% sucrose or on a mixture of 1:1 soil:vermiculite under long-day conditions (16 h light/8 h dark) in a controlled environment chamber at 22°C.

Site-Specific Mutagenesis and Generation of the Wild-Type and Mutated CSN5A-myc and CSN5B-myc Transgenic Plants

The full-length open reading frame (ORF) of *CSN5A* and *CSN5B* were amplified by RT-PCR from wild-type Arabidopsis seedlings, subcloned into pCR2.1-TOPO vector (Invitrogen, Carlsbad, CA), and sequenced. The RT-PCR reactions have been performed as previously described (Gusmaroli et al., 2002), The following gene-specific primers have been used for the amplification of *CSN5A* and *CSN5B* cDNAs: CSN5A forward primer 5′-TCGGTACCATGGAAGGTTCCTCGTC-3′; CSN5A reverse primer 5′-ACCAAGGCCTCGATGTAATCATG-3′, containing an in-frame *Stu*I fragment for the generation of the (myc9) epitope tagged CSN5A-myc ORF; CSN5B forward primer 5′-GAGGTACCATGGAGGG-TTCGTCGTC-3′; CSN5B reverse primer 5′-AGAGCAAGGCCTATATG-TAATCATAG-3′, containing an in-frame *Stu*I fragment for the generation of the (myc9) epitope tagged CSN5B-myc ORF. PCR-based site-specific mutagenesis has been performed to introduce single amino acid substitutions in the JAMM/MPN domain of CSN5A (H142A, H144A, C149A/S, D155N, and D175E/N) and CSN5B (H142A, H144A, C149A, D155N, and D175E/N), according to the instruction manual (QuickChange site-directed mutagenesis; Stratagene, La Jolla, CA). Each single amino acid substitution in the complete series of mutated CSN5A and CSN5B proteins were then confirmed by sequencing.

A myc_9 epitope tag with an in-frame 5′-*Stu*I site has been amplified, sequenced, and subsequently subcloned in frame to the complete series of wild-type and mutated *CSN5A* and *CSN5B* transgenes in pCR2.1 TOPO vectors. The fusion ORFs were then inserted into the plant binary vector pBIN19 under the control of the 35S promoter of *Cauliflower mosaic virus*. For stable transformation, the DNA constructs were electroporated into the *Agrobacterium tumefaciens* strain GV3101 (pMP90). Arabidopsis *csn5b* homozygous plants were transformed using Agrobacterium-mediated floral deep infiltration method. Transgenic plants were selected using kanamycin (100 μg/mL) (Sigma, St. Louis, MO) and gentamicin (150 μg/mL) (Sigma). The stable expression of the wild-type and mutated CSN5A-myc and CSN5B-myc versions was examined by protein blots in ~20 independent T1 resistant lines for each construct and further confirmed in their T2 progenies. The T2 progenies of transgenic lines expressing similar levels of recombinant proteins were subsequently chosen for further studies.

Protein Extraction, Gel Filtration Chromatography, and Immunoblot Analyses

Arabidopsis tissues were homogenized in extraction buffer EB1 containing 50 mM Tris-HCl, pH 7.5, 150 mM NaCl, 10 mM $MgCl_2$, 2.5 mM EDTA, 1 mM DTT, 10% glycerol, 0.1% Nonidet P-40, and freshly added protease inhibitors phenylmethylsulfonyl fluoride (PMSF) (1 mM) (Sigma) and 1× complete cocktail (Roche Molecular Biochemicals, Indianapolis, IN), phosphatase inhibitors β-glycerophosphate (60 mM), Na_3VO_4 (50 mM), and NaF (10 mM), and the metalloprotease inhibitor o-PT (2 mM). The homogenates were microcentrifuged twice for 15 min, and the supernatants were filtered through 0.2-μm filters (Gelman Sciences, Ann Arbor, MI). The protein concentrations in the supernatants were determined by Bradford assays. For gel fractionation analyses, 300 μg of total proteins were loaded onto a Superose 6 (HR10/30) gel filtration column (Amersham Pharmacia Biotech, Piscataway, NJ). The column was equilibrated with 250 mL of EB1 added with 1 mM PMSF (Sigma), 1× cocktail of inhibitors (Roche Molecular Biochemicals), 25 mM β-glycerophosphate, 10 mM Na_3VO_4, 5 mM NaF, and 2 mM o-PT. The proteins were eluted in the same buffer at a flow rate of 0.2 mL/min. All the procedures were performed at 4°C. Fractions of 0.5 mL were collected starting from the onset of the column void volume (7.0 mL) and finishing at 20 mL (26 fractions). Fractions were concentrated using StrataClean Resin (Stratagene) as previously described (Kwok et al., 1998). Equal volumes of each fraction were boiled for 5 min in 2× SDS sample buffer (Staub et al., 1996), separated by 8% SDS-PAGE, and transferred onto polyvinyledene diflouride immobilon membrane (Millipore, Bedford, MA). For direct immunoblot analyses of plant extracts, tissues were homogenized in extraction buffer EB1 as described above. Protein concentrations were determined by Bradford assays, and 20 μg of total proteins were loaded onto 8-12-15% SDS-PAGE and immunoblotted onto Immobilon membrane. In all cases in which equal loading of the samples was required, the same samples or the blots were probed with α-RPT5 to confirm the equal loading. The α-myc antibody is the monoclonal anti-9E10-myc peptide (Saijo et al., 2003). The antibody against the CSN subunits, CUL1, RPT5, and TBP, have been previously described: CSN1 (Staub et al., 1996), CSN2 (Serino et al., 2003), CSN3 (Peng et al., 2001a), CSN4 (Serino et al., 1999), CSN5 (Kwok et al., 1998), CSN6 (Peng et al., 2001b), CSN7 (Karniol et al., 1999), CSN8 (Wei et al., 1994a), CUL1 (Wang et al., 2002), RPT5 (Kwok et al., 1999), and TBP (Schwechheimer et al., 2001).

In Vivo Coimmunoprecipitation Analyses

For coimmunoprecipitation analyses, Arabidopsis tissues were homogenized in IP buffer containing 50 mM Tris-HCl, pH 7.5, 500 mM NaCl, 5 mM EDTA, 5% glycerol, and 0.1% Nonidet P-40 (IP1) and added with 1 mM PMSF and 1× complete cocktail of protease inhibitors. After centrifugation, the supernatants were filtered through 0.2-μm filters (Gelman Sciences, Ann Arbor, MI) and the protein concentrations determined by Bradford assays. For pull-down assays, 1 mg of total proteins were incubated with 30 μL of monoclonal α-myc 9E10 immobilized onto Sepharose fast flow beads (9E10 affinity matrix) (Covance, Berkeley, CA) overnight at 4°C on rotary shaker. The matrix beads were washed three times with the IP1 buffer added with 1 mM PMSF and 1× complete cocktail of protease inhibitors and twice with 20 mM Tris-HCl, pH 7.5, 150 mM NaCl, and 5% glycerol. All the wash steps were performed at 4°C for 10 min on rotary shaker followed by centrifugation at 1500 rpm. The immunoprecipitated proteins were subsequently eluted from the beads by competition with the 9E10 myc peptide (Covance) or released by boiling in 2× SDS sample buffer. The protein blot analyses of the immunoprecipitates have been performed as described above.

Scanning Electron Microscopy

Plant material was fixed overnight in a mixture of 3:1 ethanol:acetic acid by gentle shaking at 4°C, subsequently incubated in ethanol 70% for 24 h at 4°C, washed twice in ethanol 70% (1 h each), and then gradually dehydrated in an ethanol series of 70-75-80-85-95 and 100%. The dehydrated samples were dried overnight in liquid carbon dioxide (Polaron, Watford, England), gold covered in a sputter coater (Nanotech, Manchester, UK), and then observed under an ISI-SS40 scanning electron microscope (Cleaner Image, Belle Mead, NJ).

ACKNOWLEDGMENTS

We are grateful to James A. Sullivan for providing the myc_9 epitope tag vector, to Tomohiko Tsuge for the monoclonal α-myc antibody, and to Ning Wei and James Sullivan for critical reading of the manuscript. We also thank the Salk Institute Genomic Analyses Laboratory for providing the sequence-indexed Arabidopsis T-DNA insertion lines. This research was supported by grants from the National Science Foundation (MCB-0077217 and NSF 2010 MCB-0115870) to X.-W.D. G.G. was initially supported by a fellowship from Universitá degli Studi di Milano.

Received July 8, 2004; accepted August 30, 2004.

REFERENCES

Ambroggio, X.I., Rees, D.C., and Deshaies, R.J. (2004). JAMM: A metalloprotease-like zinc site in the proteasome and signalosome. PLoS Biol. **2,** 0113–0119.

Aravind, L., and Ponting, C.P. (1998). Homologues of 26S proteasome subunits are regulators of transcription and translation. Protein Sci. **7,** 1250–1254.

Busch, S., Eckert, S.E., Krappmann, S., and Braus, G.H. (2003). The COP9 signalosome is an essential regulator of development in the filamentous fungus *Aspergillus nidulans*. Mol. Microbiol. **49,** 717–730.

Castle, L., and Meinke, D. (1994). A *FUSCA* gene of *Arabidopsis* encodes a novel protein essential for plant development. Plant Cell **6,** 25–41.

Chamovitz, D.A., Wei, N., Osterlund, M.T., von Arnim, A.G., and Staub, J.M. (1996). The COP9 complex, a novel multisubunit nuclear regulator involved in light control of plant developmental switch. Cell **86,** 115–121.

Cope, G.A., and Deshaies, R.J. (2003). COP9 signalosome: A multifunctional regulator of SCF and other cullin-based ubiquitin ligases. Cell **114,** 663–671.

Cope, G.A., Suh, G.S., Aravind, L., Schwarz, S.E., Zipursky, S.L., Koonin, E.V., and Deshaies, R.J. (2002). Role of predicted metalloprotease motif of Jab1/CSN5 in cleavage of Nedd8 from Cul1. Science **298,** 606–611.

del Pozo, J.C., Dharmasiri, S., Hellmann, H., Walker, L., Gray, W.M., and Estelle, M. (2002). AXR1-ECR1-dependent conjugation of RUB1 to the Arabidopsis Cullin AtCUL1 is required for auxin response. Plant Cell **14,** 421–433.

Deshaies, R.J. (1999). SCF and Cullin/Ring H2-based ubiquitin ligases. Annu. Rev. Cell Dev. Biol. **15,** 435–467.

Dharmasiri, S., Dharmasiri, N., Hellmann, H., and Estelle, M. (2003). The RUB/Nedd8 conjugation pathway is required for early development in *Arabidopsis*. EMBO J. **22,** 1762–1770.

Doronkin, S., Djagaeva, I., and Beckendorf, S.K. (2002). CSN5/Jab1 mutations affect axis formation in the *Drosophila* oocyte by activating a meiotic checkpoint. Development **129,** 5053–5064.

Feng, S., Ma, L., Wang, X., Xie, D., Dinesh-Kumar, S.P., Wei, N., and Deng, X.W. (2003). The COP9 signalosome interacts physically with SCF^{COI1} and modulates jasmonate responses. Plant Cell **15,** 1083–1094.

Freilich, S., Oron, E., Kapp, Y., Nevo-Caspi, Y., Orgad, S., Segal, D., and Chamovitz, D.A. (1999). The COP9 signalosome is essential for development of *Drosophila melanogaster*. Curr. Biol. **9,** 1187–1190.

Fu, H., Reis, N., Lee, Y., Glickman, M.H., and Vierstra, R.D. (2001). Subunit interaction maps for the regulatory particle of the 26S proteasome and the COP9 signalosome. EMBO J. **20,** 7096–7107.

Glickman, M.H., Rubin, D., Coux, O., Wefes, I., Pfeifer, G., Cjeka, D., Baumeister, W., Fried, V.A., and Finley, D. (1998). A subcomplex of the proteasome regulatory particle required for ubiquitin-conjugate degradation and related to the COP9-signalosome and eIF3. Cell **94,** 615–623.

Gray, W.M., del Pozo, J.C., Walker, L., Hobbie, L., Risseeuw, E., Banks, T., Crosby, W.L., Yang, M., Ma, H., and Estelle, M. (1999). Identification of an SCF ubiquitin-ligase complex required for auxin response in *Arabidopsis thaliana*. Genes Dev. **13,** 1678–1691.

Gray, W.M., Hanjo, H., Sunethra, D., and Estelle, M. (2002). Role of the *Arabidopsis* RING-H2 protein RBX1 in RUB modification and SCF function. Plant Cell **14,** 2137–2144.

Groisman, R., Polanowska, J., Kuraoka, I., Sawada, J., Saijo, M., Drapkin, R., Kisselev, A.F., Tanaka, K., and Nakatani, Y. (2003). The ubiquitin ligase activity of the DDB2 and CSA complexes is differentially regulated by the COP9 signalosome in response to DNA damage. Cell **133,** 357–367.

Gusmaroli, G., Tonelli, C., and Mantovani, R. (2002). Regulation of novel members of the *Arabidopsis thaliana* CCAAT-binding nuclear factor Y subunits. Gene **283,** 41–48.

Hochstrasser, M. (1996). Ubiquitin-dependent protein degradation. Annu. Rev. Genet. **30,** 3149–3162.

Hofmann, K., and Bucher, P. (1998). The PCI domain: A common theme in three multiprotein complexes. Trends Biochem. Sci. **23,** 204–205.

Jones, D., and Candido, E.P. (2000). The NED-8 conjugating system in *Caenorhabditis elegans* is required for embryogenesis and terminal differentiation of the hypodermis. Dev. Biol. **226,** 152–165.

Karniol, B., Malec, P., and Chamovitz, D.A. (1999). *Arabidopsis FUSCA5* encodes a novel phosphoprotein that is a component of the COP9 complex. Plant Cell **11,** 839–848.

Kawakami, T., Chiba, T., Suzuki, T., Iwai, K., Yamanaka, K., Minato, N., Suzuki, H., Shimbara, N., Hidaka, Y., Osaka, F., Omata, M., and Tanaka, K. (2001). NEDD8 recruits E2-ubiquitin to SCF E3 ligase. EMBO J. **20,** 4003–4012.

Kwok, S.F., Solano, R., Tsuge, T., Chamovitz, D.A., Ecker, J.R., Matsui, M., and Deng, X.W. (1998). *Arabidopsis* homologs of a c-Jun coactivator are present both in monomeric form and in the COP9 complex, and their abundance is differentially affected by the pleiotropic *cop/det/fus* mutations. Plant Cell **10,** 1779–1790.

Kwok, S.F., Staub, J.M., and Deng, X.W. (1999). Characterization of two subunits of *Arabidopsis* 19S proteasome regulatory complex and its possible interaction with the COP9 complex. J. Mol. Biol. **285,** 85–95.

Larsen, P.B., and Cancel, J.D. (2004). A recessive mutation in the RUB1-conjugating enzyme, RCE1, reveals a requirement for RUB modification for control of ethylene biosynthesis and proper induction of basic chitinase and PDF1.2 in *Arabidopsis*. Plant J. **38,** 626–638.

Liu, C., Powell, K.A., Mundt, K., Wu, L., Carr, A.M., and Caspari, T. (2003). Cop9/signalosome subunits and Pcu4 regulate ribonucleotide reductase by both checkpoint-dependent and -independent mechanisms. Genes Dev. **17,** 1130–1140.

Lyapina, S., Cope, G., Shevchenko, A., Serino, G., Tsuge, T., Zhou, C., Wolf, D.A., Wei, N., Shevchenko, A., and Deshaies, R.J. (2001). Promotion of NEDD8-CUL1 conjugate cleavage by the COP9 signalosome. Science **292,** 1382–1385.

Lykke-Andersen, K., Schaefer, L., Menon, S., Deng, X.W., Miller, J.B., and Wei, N. (2003). Disruption of the COP9 signalosome Csn2 subunit in mice causes deficient cell proliferation, accumulation of p53 and cyclin E, and early embryonic death. Mol. Cell. Biol. **23,** 6790–6797.

Maytal-Kivity, V., Reis, N., Hofmann, K., and Glickman, M.H. (2002). MPN+, a putative catalytic motif found in a subset of MPN domain proteins from eukaryotes and prokaryotes, is critical for Rpn11 function. BMC Biochem. **3,** 28.

Miséra, S., Müller, A.J., Weiland-Heidecker, U., and Jürgens, G. (1994). The *FUSC*A genes of *Arabidopsis*: Negative regulators of light responses. Mol. Gen. Genet. **244,** 242–252.

Mundt, K.E., Liu, C., and Carr, A.M. (2002). Deletion mutants in COP9/signalosome subunits in fission yeast *Schizossacharomyces pombe* display distinct phenotypes. Mol. Biol. Cell **13,** 493–502.

Mundt, K.E., Porte, J., Murray, J.M., Brikos, C., Christensen, P.U., Caspari, T., Hagan, I.M., Millar, J.B., Simanis, V., Hofmann, K., and Carr, A.M. (1999). The COP9/signalosome complex is conserved in fission yeast and has a role in S phase. Curr. Biol. **9,** 1427–1430.

Oron, E., Mannervik, M., Rencus, S., Harari-Steinberg, O., Neuman-Silberberg, S., Segal, D., and Chamovitz, D. (2002). COP9 signalosome subunits 4 and 5 regulate multiple pleiotropic pathways in *Drosophila melanogaster*. Development **129,** 4399–4409.

Osaka, F., Saeki, M., Katayama, S., Aida, N., Toh-E, A., Kominami, K., Toda, T., Suzuki, T., Chiba, T., Tanaka, K., and Kato, S. (2000). Covalent modifier NEDD8 is essential for SCF ubiquitin-ligase in fission yeast. EMBO J. **19,** 3475–3484.

Ou, C.Y., Lin, Y.F., Chen, Y.J., and Chien, C.T. (2002). Distinct protein degradation mechanisms mediate by Cul1 and Cul3 controlling Ci stability in *Drosophila* eye development. Genes Dev. **16,** 2403–2414.

Peng, Z., Serino, G., and Deng, X.W. (2001a). A role of *Arabidopsis* COP9 complex in multifaceted developmental processes revealed by the characterization of its subunit 3. Development **128,** 4277–4288.

Peng, Z., Serino, G., and Deng, X.W. (2001b). Molecular characterization of subunit 6 of the COP9 signalosome and its role in multifaceted developmental processes in *Arabidopsis*. Plant Cell **13,** 2393–2407.

Peng, Z., Shen, Y., Feng, S., Wang, X., Chitteti, B.N., Viestra, R.D., and Deng, X.W. (2003). Evidence for a physical association of the COP9 signalosome, the proteasome and specific SCF E3 ligases *in vivo*. Curr. Biol. **13,** R504–R505.

Pepper, A., Delaney, T., Washburn, T., Poole, D., and Chory, J. (1994). *DET1*, a negative regulator of light-mediated developmental and gene expression in *Arabidopsis*, encodes a novel nuclear-localized protein. Cell **78,** 109–116.

Pintard, L., Kurz, T., Glaser, S., Willis, J.H., Peter, M., and Bowerman, B. (2003). Neddylation and deneddylation of CUL3 is required to target MEI-1/Katanin for degradation at the meiosis-to-mitosis transition in *C. elegans*. Curr. Biol. **13,** 911–921.

Ponting, C.P., Aravind, L., Schultz, J., Bork, P., and Koonin, E.V. (1999). Eukaryotic signaling domain homologues in archaea and bacteria. Ancient ancestry and horizontal gene transfer. J. Mol. Biol. **289,** 729–745.

Saijo, Y., Sullivan, J.A., Wang, H., Yang, J., Shen, Y., Rubio, V., Ma, L., Hoecker, U., and Deng, X.-W. (2003). The COP1–SPA1 interaction defines a critical step in the phytochrome A-mediated regulation of HY5 activity. Genes Dev. **17,** 2642–2647.

Samach, A., Klenz, J.E., Kohalmi, S.E., Risseeuw, G.W.H., and Crosby, W.L. (1999). The *UNUSUAL FLOWER ORGANS* gene of *Arabidopsis thaliana* is an F-box protein required for normal patterning and growth in the floral meristem. Plant J. **20,** 433–445.

Schwechheimer, C., and Deng, X.W. (2001). COP9 signalosome revisited: A novel mediator of protein degradation. Trends Cell Biol. **11,** 420–426.

Schwechheimer, C., Serino, G., Callis, J., Crosby, W.L., Lyapina, S., Deshaies, R.J., Gray, W.M., Estelle, M., and Deng, X.W. (2001). Interactions of the COP9 signalosome with the E3 ubiquitin ligase SCF^{TIR1} in mediating auxin response. Science **292,** 1379–1382.

Schwechheimer, C., Serino, G., and Deng, X.W. (2002). The COP9 signalosome and AXR1 are required for multiple E3 ubiquitin ligase-mediated processes in *Arabidopsis thaliana*. Plant Cell **14,** 2553–2563.

Seeger, M., Kraft, R., Ferrell, K., Bech-Otschir, D., Dumdey, R., Schade, R., Gordon, C., Naumann, M., and Dubiel, W. (1998). A novel protein complex involved in signal transduction possessing similarities to 26S proteasome subunits. FASEB J. **12,** 469–478.

Serino, G., and Deng, X.W. (2003). The COP9 signalosome: Regulating plant development through the control of proteolysis. Annu. Rev. Plant Biol. **54,** 165–182.

Serino, G., Su, H., Peng, Z., Tsuge, T., Wei, N., Gu, H., and Deng, X.W. (2003). Characterization of the last subunit of the COP9 signalosome: Implications for the overall structure and origin of the complex. Plant Cell **15,** 580–581.

Serino, G., Tsuge, T., Kwok, S., Matsui, M., Wei, N., and Deng, X.W. (1999). *Arabidopsis cop8* and *fus4* mutations define the same gene that encodes subunit 4 of the COP9 signalosome. Plant Cell **11,** 1967–1980.

Smalle, J., and Vierstra, R.D. (2004). The ubiquitin 26S proteasome proteolytic pathway. Annu. Rev. Plant Biol. **55,** 555–590.

Staub, J.M., Wei, N., and Deng, X.W. (1996). Evidence for *FUS6* as a component of the nuclear-localized COP9 complex in *Arabidopsis*. Plant Cell **8,** 2047–2056.

Suh, G.S., Poeck, B., Chouard, T., Oron, E., Segal, D., Chamovitz, D.A., and Zipursky, S.L. (2002). *Drosophila* JAB1/CSN5 acts in photoreceptor cells to induce glial cells. Neuron **33,** 35–46.

Tateishi, K., Omata, M., Tanaka, K., and Chiba, T. (2001). The Nedd8 system is essential for cell cycle progression and morphogenetic pathway in mice. J. Cell Biol. **155,** 571–579.

Tomoda, K., Kubota, Y., Arata, Y., Mori, S., Maeda, M., Tanaka, T., Yoshida, M., Yoneda-Kato, N., and Kato, J.Y. (2002). The cytoplasmic shuttling and subsequent degradation of p27Kip1 mediated by Jab1/CSN5 and the COP9 signalosome complex. J. Biol. Chem. **277,** 2302–2310.

Tran, H.J.T.T., Allen, M.D., Lowe, J., and Bycroft, M. (2003). Structure of the Jab1/MPN domain and its implication for proteasome function. Biochemistry **42,** 11460–11465.

Verma, R., Aravind, L., Oania, R., McDonald, W.H., Yates III, J.R., Koonin, E.V., and Deshaies, R.J. (2002). Role of Rpn11 metalloprotease in deubiquitination and degradation by the 26S proteasome. Science **298,** 611–615.

Vierstra, R.D. (2003). The ubiquitin/26S proteasome pathway, the complex last chapter in the life of many plant proteins. Trends Plant Sci. **8,** 135–142.

Wang, X., Feng, S., Nakayama, N., Crosby, W.L., Irish, V., Deng, X.W., and Wei, N. (2003). The COP9 signalosome interacts with SCF^{UFO} and participates in *Arabidopsis* flower development. Plant Cell **15,** 1071–1082.

Wang, X., Kang, D., Feng, S., Serino, G., Schwechheimer, C., and Wei, N. (2002). CSN1 N-terminal-dependent activity is required for *Arabidopsis* development but not for Rub1/Nedd8 deconjugation of cullins: A structure-function study of CSN1 subunit of the COP9 signalosome. Mol. Biol. Cell **13,** 646–655.

Wei, N., Chamovitz, D.A., and Deng, X.W. (1994a). *Arabidopsis* COP9 is a component of a novel signaling complex mediating light control of development. Cell **78,** 117–124.

Wei, N., and Deng, X.W. (1992). COP9: A new genetic locus involved in light-regulated development and gene expression in Arabidopsis. Plant Cell **4,** 1507–1518.

Wei, N., and Deng, X.W. (1996). The role of the *COP*/*DET*/*FUS* genes in the light control of *Arabidopsis* seedlings development. Plant Physiol. **112,** 871–878.

Wei, N., and Deng, X.W. (1999). Making sense of the COP9 signalosome. A regulatory protein complex conserved from *Arabidopsis* to humans. Trends Genet. **15,** 98–103.

Wei, N., and Deng, X.W. (2003). The COP9 signalosome. Annu. Rev. Cell Dev. Biol. **19,** 261–286.

Wei, N., Kwok, S.F., von Arnim, A.G., Lee, A., McNellis, T.W., Piekos, B., and Deng, X.W. (1994b). *Arabidopsis* COP8, COP10, and COP11 genes are involved in repression of photomorphogenic development in darkness. Plant Cell **6,** 629–643.

Wei, N., Tsuge, T., Serino, G., Dohmae, N., Takio, K., Matsui, M., and Deng, X.W. (1998). The COP9 complex is conserved between plants and mammals and is related to the 26S proteasome regulatory complex. Curr. Biol. **8,** 919–922.

Wolf, D.A., Zhou, C., and Wee, S. (2003). The COP9 signalosome: An assembly and maintenance platform for cullin ubiquitin ligases? Nat. Cell Biol. **5,** 1029–1033.

Wu, K., Chen, A., and Pan, Z.Q. (2000). Conjugation of Nedd8 to CUL1 enhances the ability of the ROC1–CUL1 complex to promote ubiquitin polymerization. J. Biol. Chem. **275,** 32317–32324.

Xu, L., Liu, F., Lechner, E., Genschik, P., Crosby, W.L., Ma, H., Peng, W., Huang, D., and Xie, D. (2002). The SCFCOI1 ubiquitin-ligase complexes are required for jasmonic response in *Arabidopsis*. Plant Cell **14,** 1919–1935.

Yang, X., Menon, S., Lykke-Andersen, K., Tsuge, T., Xiao, D., Wang, X., Rodriguez-Suarez, R.J., Zhang, H., and Wei, N. (2002). The COP9 signalosome inhibits $p27^{KIP1}$ degradation and impedes G1-S phase progression via de-neddylation of SCF Cul1. Curr. Biol. **12,** 667–672.

Yao, T., and Cohen, R.E. (2002). A cryptic protease couples deubiquitination and degradation by the proteasome. Nature **419,** 403–407.

Zhao, D., Yu, Q., Chen, M., and Ma, H. (2001). The *ASK1* gene regulates B function gene expression in cooperation with UFO and LEAFY in *Arabidopsis*. Development **128,** 2735–2746.

Zhou, C., Seibert, V., Geyer, R., Rhee, E., Lyapina, S., Cope, G., Deshaies, R., and Wolf, D.A. (2001). The fission yeast COP9/signalosome is involved in cullin modification by ubiquitin-related Ned8p. BMC Biochem. **2,** 7–17.

Zhou, C., Wee, S., Rhee, E., Naumann, M., Dubiel, W., and Wolf, D.A. (2003). Fission yeast COP9/signalosome suppresses cullin activity through recruitment of the deubiquitylating enzyme Ubp12p. Mol. Cell **11,** 927–938.